

Oxidative Dehydrogenation of Propane and Butane to
Olefins using Co(5)MgAlO Catalyst

By

NAMPE MAJOE

submitted in accordance with the requirements for the degree of

MASTER OF TECHNOLOGY

In the subject

CHEMICAL ENGINEERING

at the

UNIVERSITY OF SOUTH AFRICA

SUPERVISOR: **PROF CM MASUKU**

CO-SUPERVISOR: **DR J GORIMBO**

SEPTEMBER: 2019

DECLARATION

Name: Nampe Majoe

Student number: 57579350

Degree: Master of Technology in Engineering Chemical

Title: Oxidative Dehydrogenation of Propane and Butane to Olefins using Co(5)MgAlO Catalyst

I declare that the above dissertation is my own work and that all the sources that I have used or quoted have been indicated and acknowledged by means of complete references. I further declare that I submitted the dissertation to originality checking software and that it falls within the accepted requirements for originality. I further declare that I have not previously submitted this work, or part of it, for examination at Unisa for another qualification or at any other higher education institution.



2019-10-03

Signature:

Date:

ABSTRACT

Olefins have enjoyed many uses in a wide variety of industries, from car manufacturing to energy production. Energy consuming processes of catalytic dehydrogenation, turning paraffins into olefins, has been commercialised since the early 20th century, while catalytic oxydehydrogenation of paraffins to olefins is still in prototype stages. The conflict between kinetic and thermodynamic yield constraints, has delayed the commercialisation of this process. The solution to achieving the relevant process route is exploitation of the right catalyst at moderate temperatures and pressures. Co₅MgAlO is studied under atmospheric pressure and 350°C temperature, to dehydrogenate propane and butane to olefins using oxygen as a reactant. Thermodynamic models showing how many reaction routes are possible under atmospheric pressure were explored. Experimental results for butane to air at ratio of 1:0.8 and 1:1.2 hydrocarbons to air gave better selectivity of 1-butene which was more than 12%. When compared with propane at similar reaction ratios the reaction favoured CO₂ at selectivity of more than 95%.

Keywords; Paraffins to Olefins Conversion, Propane and Butane Yield, Thermodynamic models, Paraffin Dehydrogenation Routes, Cobalt-Magnesium on Aluminium Oxide Catalyst.

ACKNOWLEDGEMENTS

It is my pleasure firstly to acknowledge my wife Dineo and son Thuto for letting me be when I didn't need to be disturbed and sometimes for hours.

Second acknowledgement goes to both my supervisors, Prof CM Masuku for his theoretical insight and lot of discussions around thermodynamics and Dr J Gorimbo for his attention to detail when it comes to experimental work.

Third acknowledgment goes to my work colleagues at Ekurhuleni East TVERT College for their words of encouragement to go on.

To my fellow students at University of South Africa, Florida Campus; I say to you all thank you.

Above all thing I would like to thank the Lord of Mount Zion for spiritual guidance and protection during all these years.

PRESENTATIONS AND PUBLICATIONS

Parts of the data contained in this dissertation will be written in paper format to be submitted to peer reviewed journals. Some of the data was presented (orally) and are outlined in this section.

Conference Presentations

- N. Majoe, CM Masuku, J Gorimbo, Oxy Dehydrogenation of Paraffins to Olefins Using Co_5MgAlO Catalyst, Oral Presentation, American Institute of Chemical Engineers (AIChE) 2018 Spring Meeting and 14th Global Congress on Process Safety. Orlando World Center Marriott, FL., USA

CONTENTS

Declaration	2
Abstract	3
Acknowledgements	4
Contents	6
Chapter 1: Introduction	11
1.1. Executive summary	11
1.2. Why use Volatile Organic Compound (VOC)?	12
1.3. Aims of the Projects	12
1.4. Research objectives	12
Chapter 2: Literature Review	14
2.1. Background	14
2.2. Current methods of olefin production	15
2.2.1. Steam Cracking	15
2.2.2. Catalytic Cracking	18
2.2.3. Catalytic modelling of dehydrogenation	19
2.2.4. Dehydrogenation Catalysts	22
2.3. Oxy-dehydrogenation	23
2.3.1. Key factors in selective ODH of light alkanes (paraffins)(Gavani, 1999)	24
2.3.2. Key bulk and surface properties of catalysts which affect performance	24
2.3.3. Overview of different catalysts used for oxidation of propane to propene	25
2.4. Concluding Remarks	29
Chapter 3: Fundamental thermodynamics analysis	31
3.1. Introduction	31
3.2. Fundamental thermodynamics	31
3.2.1. Propane oxidative dehydrogenation to propene	35
3.2.2. Propane oxidative dehydrogenation to other routes	39
3.2.3. Butane oxidative dehydrogenation to other olefins	40
3.3. Results and Discussions	41

3.3.1	Propane oxy-dehydrogenation routes	41
3.3.2.	Butane oxy-dehydrogenation to butylene and other hydrocarbons	46
3.4.	Concluding Remarks	47
	Chapter 4: Experimental Details	48
4.1.	Introduction	48
4.2.	Materials used	48
4.3.	Catalytic preparation	48
4.4.	Characterization	49
4.5.	Experimental Condition.	50
4.6.	ODH Reactors	51
4.7.	Catalyst loading into the reactor	51
4.8.	Experimental set-up	52
4.9.	Experimental method	54
4.9.1.	Catalyst activation procedure	54
4.9.2.	ODH reaction runs	55
	Chapter 5: Results and Discussions	56
	Chapter 6: Conclusion	63
	References	66
	Appendix	70

List of figures

Figure1: Principal arrangement of cracking furnace (Levels, 2002).	16
Figure 2: Temperatures required in achieving 10 and 40% conversion of $C_2 - C_{15}$ n-paraffins at 1 atm (Bhasin, 2001).	19
Figure 3: Fluid-bed catalytic cracking with product separation (Levels, 2002).	19
Figure 4: equilibrium constant for $C_2 - C_{16}$ dehydrogenation at 500 °C (Bhasin, 2001).	21
Figure 5: Gibbs free energy and spontaneity	32
Figure 6: ΔG vs. G° : ΔG is plotted on a vertical axis for two hypothetical reactions having opposite signs of ΔG° .	32
Figure 7: Simplified Oxydehydrogenation Gibbs free energy vs Quotient of the reaction graph	35
Figure 8: Relationship between Temperature (T_b) versus propene selectivity %	42
Figure 9: Relationship between Temperature (T_b) versus propene selectivity % with catalysts plots.	42
Figure 10. Relationship between propane conversion and propene selectivity (Kung, 1997)	43
Figure 11: Relationship between Temperature (T_b) versus other hydrocarbons selectivity %	44
Figure 12: Relationship between Temperature (T_b) versus undesired routes selectivity %	45

Figure 13: Relationship between Temperature (T_b) versus olefins routes selectivity %

47

Figure 14: Dismantled reactor photograph. (Gorimbo, 2016)

51

Figure 15: ODH reactor with loaded catalyst (Gorimbo, 2016)

52

Figure 16: Laboratory scale ODH rig flow scheme of fixed reactor

53

Figure 17: XRD patterns of Co_5MgAlO

56

Figure 18: The TGA profile for the Co_5MgAlO catalyst

57

Figure 19: H_2 – TPR profiles of Co_5MgAlO catalyst

58

Figure 20: Nitrogen adsorption/desorption isotherms profile at $-195\text{ }^\circ\text{C}$ Co_5MgAlO catalyst

59

Figure 21: Reaction runs on thermodynamic plots for CO_2 cut

60

Figure 22: Reaction runs on thermodynamic plots for olefin cut.

62

List of tables

Table1: Yields from propane cracking with various residence times (wt%) (Levels, 2002)

17

Table 2: Vanadium catalysts efficiencies with respect to temperature and V content for Propane conversion to Propene

26

Table 3: Platinum catalysts efficiencies with respect to temperature and Pt content for Propane conversion to Propene

27

Table 4: MMgAlO (M = Mn, Fe, Co, Ni, Cu, Zn) catalysts efficiencies with respect to temperature for Propane conversion to Propene	28
Table 5: Co _(x) MgAlO catalysts efficiencies with respect to temperature and Co content for Propane conversion to Propene	29
Table 6: Table of % conversions (x) and Value of K_p	39
Table 7: Table of reaction (1 – 8) H_a and G_a with K_p	40
Table 8: Table of reaction (9 – 11) H_a and G_a with K_p	41
Table 9: Temperature T_b of reaction for % conversion x of propane to propene	41
Table 10: % selectivity and reaction temperatures for olefins and alcohol routes	43
Table 11: % selectivity and reaction temperatures for undesired routes	43
Table 12: Product selectivities and conversions for Mg orthovanadate and Mg pyrovanadate (Kung, 1992)	44
Table 13: % selectivity and reaction temperatures for olefins routes	46
Table 14: Reaction flow rates for Paraffins and Oxygen for run 1 – 4.	55
Table 15: Conversion % of Olefins and Oxygen and Product selectivity % for Oxidative dehydrogenation reaction	61
Table 16: Product selectivities and conversions for Mg orthovanadate and Mg pyrovanade (Kung, 1992)	64

Chapter 1: Introduction

1.1. Executive summary

M King Hubert came up with a life cycle model for automotive fuel production in the mid-1950s termed Hubert's model (Degirmenci, 2005). From the life cycle model, his prediction was that fuel in the U.S will peak around 1969, which happened in 1970. The extension of his model proposes that fuel will be depleted by around 2060 (Degirmenci, 2005). Crisis in the oil market has produced some deterioration in world economic activity and has created a need to replace fossil fuel with more renewable sources of energy (Busto, 2008).

Petrochemical industries continue to emit volatile organic compounds (VOC), which contribute to atmospheric pollution. Light paraffins ($C_3 - C_4$) are among the most known VOC emissions due to their presence in crude oil (Urdâ, 2009). These paraffins could be separated from other VOC and converted into olefins, which can later be used as a feed for production of petroleum and polyethylene products.

The challenge facing scientist and engineers in this process is the C – H bonds in light paraffin which is very strong (425 kJ/mol) and contain no functional group, magnetic moment or polar distribution to induce chemical reaction (Holmen, 2009). To be able to break the paraffin single bond and rearrange it into olefins double bond, it will either require high energy (temperature) or effective catalytic process. High temperature at long reaction times also comes with negative impact as they cut the hydrocarbons and produce carbon mass consisting of CH_4 and CO_x . These challenges open more research into better routes for production of olefins from light paraffins at moderate temperature.

From olefins there are numerous other compounds which can be derived, and there is an extensive research and industrial modification for production of motor fuel from olefins.

1.2. Why use Volatile Organic Compounds?

Petrochemical refineries and petrochemical plants are large industries, where most of the VOCs are derived from petroleum fractions (Odabasi, 2003). Several effects of VOCs are recognised, such as their contribution to stratosphere ozone depletion, troposphere photochemical ozone formation, toxic and carcinogenic human health effects and enhancement of global greenhouse effect (Lo, 2004; Odabasi, 2003). Many studies on effects of VOCs on human health have been reported elsewhere (Mølhave, 1986; 1991).

It is evident that conversions of VOCs to more useful materials such as petroleum and polyethylene via olefins are very important to both energy industry, health and the environment. Use of catalyst to convert the VOCs into olefins will be looked at in more detail in subsequent sections.

1.3. Aims of the Projects

The main aim of this dissertation is to investigate the benefits and limitations of $\text{Co}_{(5)}\text{MgAlO}$ as a suitable catalyst for oxidative dehydrogenation of light paraffins (propane and butane) into olefins at moderate temperatures and pressures. Pros and cons of commercialised thermal dehydrogenation process will also be theoretically reviewed and compared to oxidative dehydrogenation.

1.4. Research objectives

- To determine the ideal temperature, pressure and space velocity for paraffins oxidative dehydrogenation to olefins using $\text{Co}_{(5)}\text{MgAlO}$ as catalyst.

- To determine the degree of nano-particle loading of $\text{Co}_{(5)}\text{MgAlO}$ catalyst for olefins production.
- Measure and compare in terms of selectivity and yield thermodynamic calculations between propane and butane.
- Measure and compare performance of the catalyst in terms of selectivity and yield with known literature data for catalytic dehydrogenation.

Chapter 2: Literature Review

2.1. Background

Efficient transformation of paraffinic feedstock into more valuable olefins or reactive compounds continues to represent a significant academic challenge with strong economic benefits (Lorkovic, 2004). The formation of olefins is attained by dehydrogenation process, the initial activation of C–H bond in alkanes using a transition metal as catalyst. Dehydrogenation of paraffins is an energy intensive reaction that requires relatively high temperature to obtain high yields of olefins (Marcu, 2008). However, thermal dehydrogenation process gives lower yields due to coke formation. Deactivation of catalyst at higher temperatures is also a disadvantage. The oxidative dehydrogenation of paraffin over a catalyst could come as a solution (Marcu, 2008).

Interest in conversion of light alkanes to valuable olefins by means of oxidation has been growing in recent years due to the possibility of having new products with less environmental impact and less cost (Cavani, 1999). The main problem with most redox type catalysts in oxidative dehydrogenation is that olefins yields do not exceed 30%; the reason for these low yields is due to the effective activation of alkenes produced after dehydrogenation (Leon, 2002). These alkenes are found to adsorb strongly on these catalysts, inducing the deep oxidation of the desired product.

Oxy-dehydrogenation has mostly been studied using catalyst containing vanadium and most currently platinum. It has been reported that oxy-dehydrogenation at ± 1000 °C and very short residence time over Pt and Pt-Sn catalysts can produce ethylene in higher yields than in steam cracking (Bhasin, 2001). However, there are many issues regarding safety due to volatility of hydrocarbon and oxygen at high temperatures and other process concerns that need to be addressed at high temperatures.

At 600°C it is reported that Oxy-dehydrogenation of propane using $\text{Co}_{(5)}\text{MgAlO}$ as a catalyst could convert 15.4% propane with product selectivity of 67.5% propene, 29.5% cracking products and 3% $\text{CO}_{(x)}$ (Marcu, 2012). This catalyst was however not tested for conversion of butane to olefins.

2.2. Current methods of olefin production.

Most of the short chain olefins manufactured are converted directly or indirectly to polymers and others to motor fuel and synthetic products. The demand for polymers, motor fuel and synthetic products is increasing, and so these short chain olefins, mostly ethene and propene, follow this demand (Levels, 2002). William Burton as chemist employed by Standard Oil in 1913; invented a thermal cracking process for breaking up large non-volatile hydrocarbons into gasoline (Britannica, 2015). In 1930s Dr Hans Tropsch (of the Fischer-Tropsch process) headed a research work by Dr Julian M. Mavity which further enhanced the process by addition of a catalyst to thermal cracking in order to lower the required temperature (Thomas, 2009).

Almost all the light olefins (C_3 and C_4) universal production is carried out by three commercialised processes: Thermal cracking (pyrolysis or steam cracking), catalytic cracking and catalytic dehydrogenation. A brief literature review of these processes is given below.

2.2.1. Steam Cracking

Most of nowadays alkenes production is derived from thermal cracking of petroleum hydrocarbon, most often LPG and naphtha, with steam; the process is normally called pyrolysis or steam cracking (Levels, 2002). The main product of steam cracking is ethene, propene and limited amounts of higher olefins are by products from this process.

Process Flow

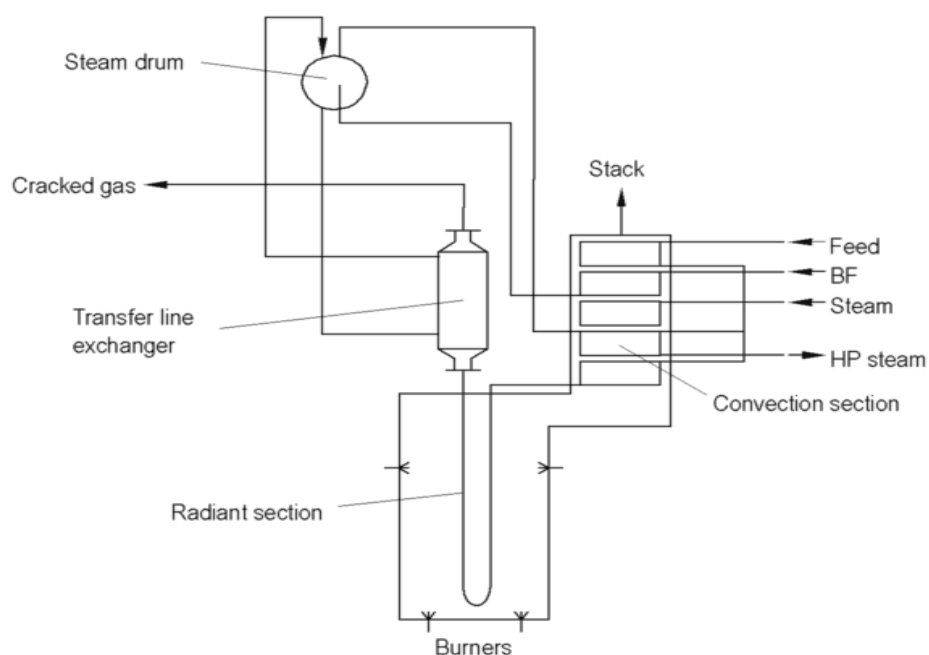


Figure1: Principal arrangement of cracking furnace (Levels, 2002).

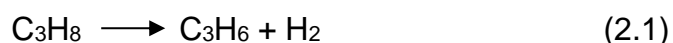
From Figure1 above of a steam cracking reactor, a hydrocarbon stream is warmed by heat exchanger against the flue gas in the convection section. It is then mixed with steam and further heated to cracking temperature of about 500 – 680 °C. The stream then goes to fire tube reactor where under a controlled reaction time, temperature profile and partial pressure, it is heated to further 750 – 875 °C for 0.1 – 0.5 seconds. During this residence time, the feedstock of hydrocarbon is broken down into smaller molecules: ethylene, other olefins and di-olefins are the major products. The reaction products then leave through the radiant tube at 800 – 850 °C and are cooled to 550 – 650 °C within 0.02 – 0.1 sec to prevent further breakdown of highly reactive products by secondary reactions (Levels, 2002). The product stream composition of propane cracking is listed below.

Table1: Yields from propane cracking with various residence times (wt%) (Levels, 2002)

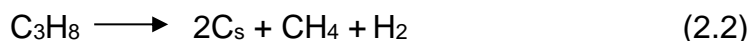
Conversion, kg/kg	90.02	90.035	89.926	89.983
Steam dilution, kg/kg	0.3	0.3	0.3	0.3
Residence time	0.445	0.3337	0.1761	0.1099
H ₂	1.51	1.55	1.61	1.68
CO	0.04	0.04	0.03	0.04
CO ₂	0.01	0.01	0.01	0.01
H ₂ S	0.01	0.01	0.01	0.01
CH ₄	23.43	23.27	22.28	22.4
C ₂ H ₂	0.46	0.51	0.59	0.82
C ₂ H ₄	37.15	37.51	38.05	38.59
C ₂ H ₆	3.06	2.8	2.37	1.96
C ₃ H ₄	0.52	0.57	0.65	0.89
C ₃ H ₆	14.81	14.82	15.01	15.27
C ₃ H ₈	9.97	9.96	10.07	10.01
C ₄ H ₄	0.08	0.08	0.09	0.11
C ₄ H ₆	2.85	2.9	2.98	2.99
C ₄ H ₈	1	1	1.02	1.09
C ₄ H ₁₀	0.04	0.04	0.05	0.05
Benzene	2.15	2.12	2.02	1.8
Toluene	0.43	0.4	0.36	0.28
Xylenes	0.05	0.05	0.04	0.03
Ethylbenzene	0.01	0.01	0.01	0
Styrene	0.21	0.2	0.18	0.15
Pyrolysis gasoline	1.27	1.26	1.27	1.24
Pyrolysis fuel oil	0.94	0.89	0.76	0.58
Sum	100	100	100	100

Reaction mechanism

Olefin production which is a basis chemical for polyethylene products and production of gasoline is achieved through steam cracking of light paraffins. For C₂ – C₅ the primary reaction is dehydrogenation (Schmidt, 2000). An example with ethane is given in equation 2.1 below.



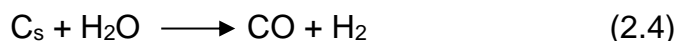
The reaction requires a residence time of 0.1 to 1s and is endothermic. Hydrogen and methane by-products are used as fuel to drive the chemistry. Equation 2.2 illustrates the by-product (Fuel) production.



There is also undesired reaction in pyrolysis that form coke (C_s) for higher residence time (see equation 2.3).



Adding steam to the process slows down the formation of coke according to this reaction illustrated by equation 2.4;



Steam cracking technology for Olefin production needs great investment and higher reaction temperature.

2.2.2. Catalytic Cracking

Direct dehydrogenation is an endothermic reaction, it is limited in terms of equilibrium and the reaction requires special catalysts for selectivity, because a high temperature

favours side reactions and coke formation (Nawaz, 2013). Below is an example of catalytic cracking flow diagram (fluid-bed catalytic cracking) with product separation.

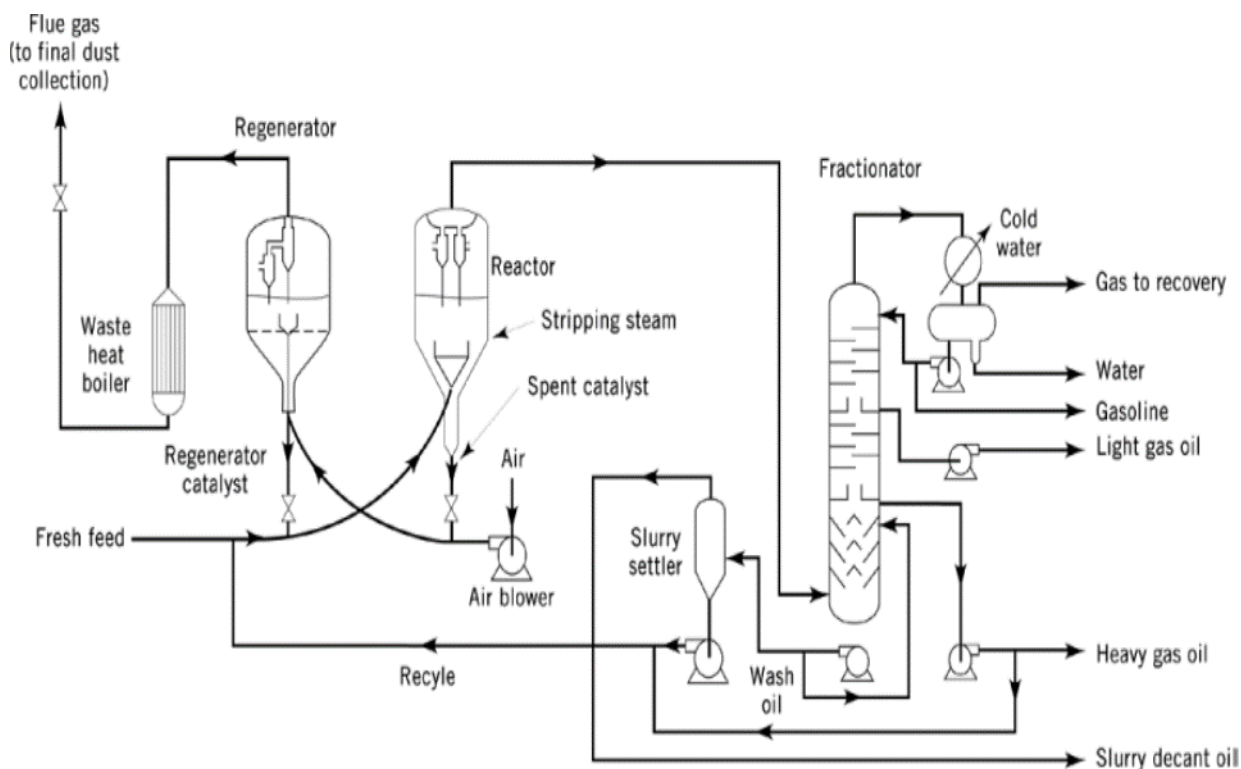


Figure 3: Fluid-bed catalytic cracking with product separation (Levels, 2002).

The catalytic cracking technique because of its ability to lower the reactor temperature is considered to be one of the most effective ways in production of olefins (Jiang, 2008). From 1940s Haensel (Bhasin, 2001) demonstrated that Pt-based catalyst had high active site for dehydrogenation of paraffins to olefins. This approach of dehydrogenation of light paraffins to olefins was first commercialised in the middle of 1960s for the production of biodegradable detergents from long chain linear olefins (Bhasin, 2001). By 1999, there were more than 30 commercialised Pt-based catalysts for dehydrogenation of long chain paraffins to olefins (Bhasin, 2001). Long chain paraffins are easier to dehydrogenate and they only require typically below 500°C temperatures. While this is the case for long chains paraffins dehydrogenation, it is not the same with short chains. Figure 2 below shows temperatures required to achieve 10 and 40% conversion of C₂ – C₁₅ n-paraffins at atmospheric pressure (Bhasin, 2001).

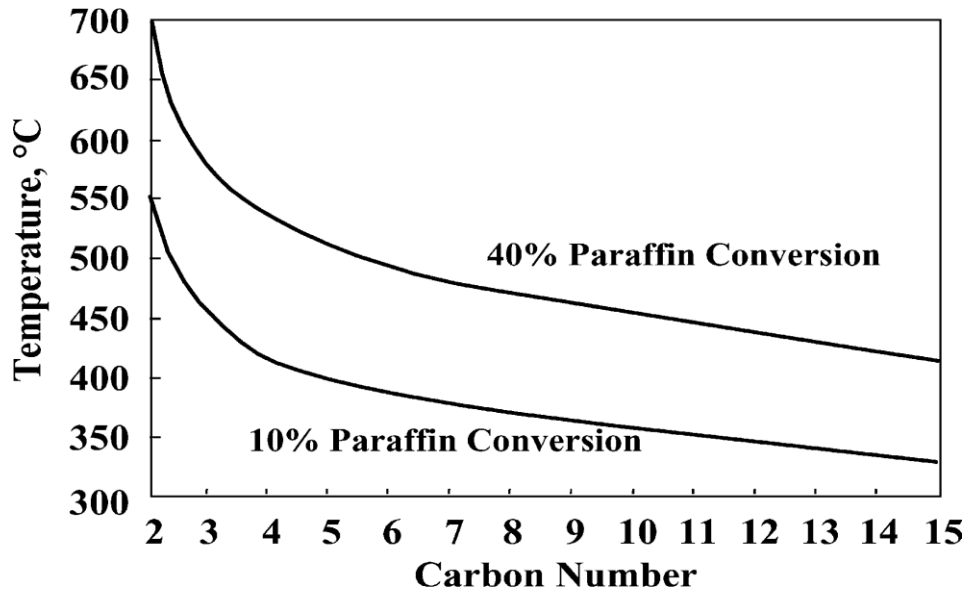


Figure 2: Temperatures required in achieving 10 and 40% conversion of C₂ – C₁₅ n-paraffins at 1 atm (Bhasin, 2001).

2.2.3. Catalytic Modelling of Dehydrogenation

Paraffins dehydrogenation is an endothermic reaction and that by Le Chatelier's principle is limited by chemical equilibrium. High conversions will require high temperatures and lower pressures (Bhasin, 2001). Therefore, the production of mono-olefins can be expressed by this equation;

$$x_e^2 = \frac{K_p}{K_p + P} \quad (2.5)$$

Where x_e is the equilibrium conversion, P the total absolute pressure and K_p is the equilibrium constant for dehydrogenation reaction (Bhasin, 2001). Rate of paraffin conversion (x) and mono-olefin production (sx) are given using Equations 2.6 and 2.7 below as shown by Bhasin (2001);

$$\frac{dx}{dt} = f_1(k_i, K_i p_j) \quad (2.6)$$

$$\frac{d(sx)}{dt} = f_2(k_i, K_i p_j) \quad (2.7)$$

Where s is the selectivity to n -mono-olefins, t is the contact time, f is the rate function, k_j is the rate constant for reaction step i , K_i is the equilibrium constant for reaction step i , and p_i is the partial pressure of the j compound.

The relationship between selectivity and conversion was then derived from equation 2.6 and 2.7 as follows;

$$\frac{d(sx)}{dx} = \frac{f_2(k_i, K_i, p_i)}{f_1(k_i, K_i, p_i)} \quad (2.8)$$

The k_i and K_i are function of temperature; and p_j is a function of conversion, total pressure (P), and feed ratio (R). Therefore, Eq (2.8) can be written as

$$\frac{d(sx)}{dx} = \frac{f_2[k_i(T), K_i(T), x, P, R]}{f_1[k_i(T), K_i(T), x, P, R]} \quad (2.9)$$

Eq. 2.9 is the ratio of two functions, where the rate function becomes relative values and can be expressed as $k_i(T)/k_0(T)$, where $k_0(T)$ is the rate constant for the forward reaction of paraffin dehydrogenation to mono-olefins. Therefore, equation 2.9 can be written in a functional form in F as follows:

$$\frac{d(sx)}{dx} = F \left[\frac{k_i(T)}{k_0(T)}, K_i(T), x, P, R \right] \quad (2.10)$$

Equation 2.10 clearly indicates that selectivity is a function of conversion for the catalyst used (relative rate constant) and the given reaction conditions (temperature, pressure, feed ratio). Therefore, the relationship between selectivity and conversion can be simulated according to equation 2.10, if rate functions, relative rate constant and equilibrium constants are known (Bhasin, 2001). Selectivity decreases as the conversion increases because n -mono-olefins are consecutively converted into by-product. Selectivity decreases sharply as conversion approaches equilibrium because the main dehydrogenation process is limited by equilibrium, but other reactions

continues. Figure 3: shows equilibrium constant for C₂ – C₁₆ dehydrogenation at 500 °C (Bhasin, 2001).

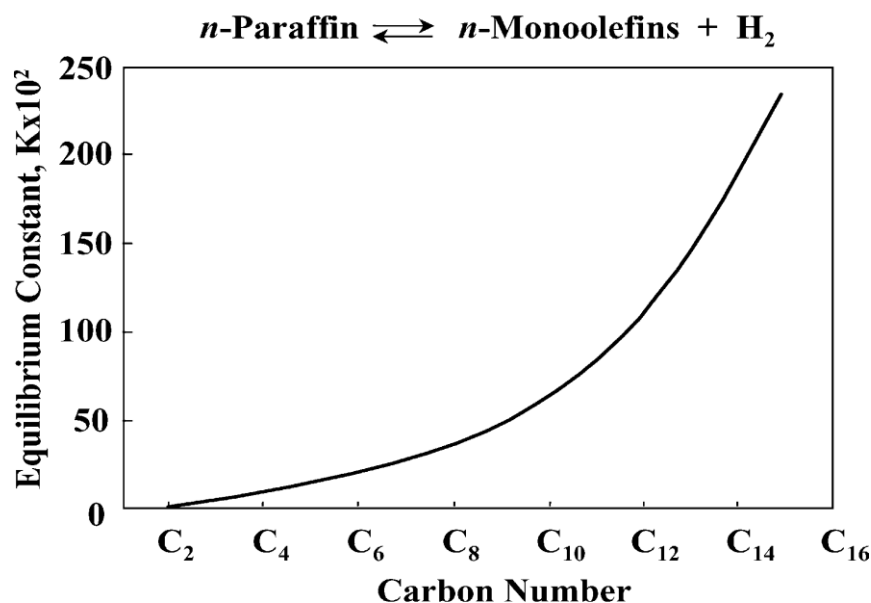


Figure 4: equilibrium constant for C₂ – C₁₆ dehydrogenation at 500 °C (Bhasin, 2001).

2.2.4. Dehydrogenation Catalysts.

The employment of the right catalyst allows high reaction rates and selectivity, but from Subsection 2.2.3 we have seen that when increasing conversion, the selectivity drops off. The main types of catalysts reported in the patent and scientific literature are as follows (Sanfilippo, 2006);

- (a) Group VIII metals (basically supported platinum/tin, with promoters),
- (b) Chromium oxides on Alumina or Zirconia, with promoters,
- (c) Fe oxides, with promoters,
- (d) Ga, supported oxide or included in zeolite,

However, these catalysts have not gone without limitations due to the nature of dehydrogenation reactions. Equilibrium conversion is limited by thermodynamics and increases with temperature (Sanfilippo, 2006). Because the separation of unreacted

paraffins from the product is costly, the conversion percentage should be high, thereby requiring temperatures exceeding 550°C. Light paraffins require high temperature and the higher temperature equate to more engineering difficulties (Sanfilippo, 2006).

Limitations of dehydrogenation catalysts as temperature gets higher are:

- High temperature means more side reactions, eventually leading to low yields,
- Coke formation is critical to any catalyst. Periodical catalyst regeneration is therefore necessary to restore the activity of catalyst.
- The equilibrium activity increases by lowering the pressure; therefore some technologies operate at a pressure below 1 atm (vacuum, H₂ or steam dilution) to get higher driving force.
- Endothermic reaction (about 125 kJ/mol of extracted hydrogen) results in a higher heat demand on weight basis for production of olefins.

All the above limitations mandate a synergetic process design and the nature of catalyst as well as the reactor design.

Oxidative dehydrogenation investigates the possibility of a new process with extensive possible benefits.

2.3. Oxy-dehydrogenation

A huge amount of papers aimed at the oxidative dehydrogenation of paraffins indicates both scientific and industrial interest for alternatives to catalytic and thermal dehydrogenation which suffers from energetic drawbacks (Gavani, 1999). However, as mentioned in *thermal dehydrogenation*, this process gives lower yields due to coke formation. Deactivation of catalyst at higher temperatures is also a challenge. The oxidation dehydrogenation (ODH) of paraffins over a catalyst could come as a solution.

The main problem associated with ODH catalysts involves a decrease in olefin selectivity as the alkane conversion increases (Lemonidou, 1998). The alkenes are more reactive than alkanes and on the surface of the catalyst they might undergo a second oxidation to CO_x (Lemonidou, 1998). There are several factors that need to be studied before ODH catalyst can be selected. Some of these are the key factors and surface properties as outlined below;

2.3.1. Key factors in selective ODH of light alkanes (paraffins)(Gavani, 1999)

- 2.3.1.1. The role of oxygen to be adsorbed and the importance of the mode of the alkane adsorption
- 2.3.1.2. The mechanism of activation of the C – H bond and the stability of the products.
- 2.3.1.3. The contribution of homogeneous reactions, for applications which need temperatures more than 400 – 450°C and the effect of core adsorbates in making possible the dissociative adsorption of saturated hydrocarbons.

A better comprehension of the above factors means a better understanding of the total process of alkane transformation,

2.3.2. Key bulk and surface properties of catalysts which affect performance

- 2.3.2.1. *Surface of the catalyst.* The nature of the active site and how the surface is affected by the bulk features and specifically;
 - Surface acidity role

2.3.2.2. *The structure of catalyst.*

- Redox properties of the metal in oxide-based catalyst and the metal – oxygen bond strength.
- The interaction between the support and the active site in modifying the catalytic properties.

2.3.2.3. *Site isolation theory* – explains the importance of number of surface oxidising sites statistically controlled in order to favour selective oxidation reactions over combustion reactions.

It should be noted that these aspects are applied in most cases to hydrocarbon oxidation, not only specific for light paraffins transformations to olefins.

2.3.3. *Overview of different catalysts used for oxidation of propane to propene*

2.3.3.1. *Vanadium supported catalysts.*

Vanadium oxides catalysts are well researched to give better selective oxy-dehydrogenation of light paraffins, but their catalytic properties depend on the metal oxide support and vanadium content (Trifiro, 1997). It has been proposed that the presence of isolated tetrahedral V^V species is responsible for high selectivity to olefins and that the selectivity drastically decreases for vanadium loading above 2 wt.% (Grzybowska, 2006). V_2O_5/MgO has shown high efficiency but failed to avoid total oxidation of paraffin molecules (Marcu, 2011). The below table shows different vanadium catalysts efficiency at certain temperatures;

Table 2: Vanadium catalysts efficiencies with respect to temperature and V content for Propane conversion to Propene

Catalyst	Conversion	Selectivity	Temperature	V content	Author
VSi β	16.5%	62%	470°C	1.22%	Grzybowska, 2006
VTiO ₂	10%	42%	500°C	5%	Lemonidou, 2005
VAI ₂ O ₃	10%	22%	500°C	14%	Lemonidou, 2005

2.3.3.2. *Platinum catalysts*

Platinum (Pt) is an element required in small quantities (ca. 0.5 wt.%) for commercial dehydrogenation of paraffins if it is dispersed evenly to achieve high selectivity (Sun, 2015). Very high selectivity to olefins has been reported for oxidation of light paraffins over Pt-coated foam monoliths, operating adiabatically at extremely short contact time (1 – 10 ms) (Beretta, 2001). Oxidative dehydrogenation over Pt catalyst is achieved at high temperatures (700 – 1000°C), in spite of the homogeneous contributions at high temperatures explaining conversions, the heterogeneous contributions are used to explain the higher selectivity to olefins (Beretta, 2001). This is shown to be a considerable improvement with respect to performances of selective oxidation catalysts, which tend to have loss of selectivity at increased conversions (Forzatti, 2001). Elsewhere a specially designed tubular micro-reactor was used to test performance of Pt supported onto corundum micro-monoliths in the reaction of propane oxidative dehydrogenation at short contact times (Sadykov, 2000). The results of the experiment are tabulated below;

Table 3: Platinum catalysts efficiencies with respect to temperature and Pt content for Propane conversion to Propene (Sadykov, 2000)

Catalyst	Conversion	Selectivity	Temperature	Pt content
P – 1	63%	17.5%	835°C	3%
P – 2	47%	26.4%	850°C	2%
P – 3	62%	20.6%	840°C	2%
P – 4	33%	25.3%	880°C	0.5%

2.3.3.3. *Other catalysts*

Large developments of transition metal oxides mostly vanadium has been known to give better results for the oxidative dehydrogenation of light paraffins (Marcu, 2011). Mg/V/O catalysts have been the object of investigation for many years, because the conversions can be achieved for propane conversions in temperatures ranging between 500 – 600 °C (Trifiro, 1995). Elsewhere it was also reported that the VMgAlO was more active than mostly referenced VMgO in oxidative dehydrogenation of propane (Marcu, 2011). More transitional metals MMgAlO (M = Mn, Fe, Co, Ni, Cu, Zn) were then investigated and the table below shows the results of propane conversion and olefins selectivity as a function of temperature (Marcu, 2011).

Table 4: MMgAlO (M = Mn, Fe, Co, Ni, Cu, Zn) catalysts efficiencies with respect to temperature for Propane conversion to Propene (Marcu, 2012)

Catalyst	Conversion (%)	Selectivity (%)	Temperature
MnMgAlO	2.7 – 12.9	73.4 – 70.3	450°C – 600°C
FeMgAlO	0.9 – 7.9	36.0 – 47.4	450°C – 600°C
CoMgAlO	1.5 – 15.4	92.5 – 67.5	450°C – 600°C
NiMgAlO	1.0 – 12.4	86.4 – 66.3	450°C – 600°C
CuMgAlO	2.5 – 11.0	26.1 – 11.1	450°C – 600°C
ZnMgAlO	0.6 – 9.8	76.7 – 64.0	450°C – 600°C
MgAlO	0.8 – 7.7	10.8 – 25.6	500°C – 600°C

2.3.4. CoMgAlO catalyst background

From 2.3.3, it is evident that CoMgAlO is a better catalyst at 600°C, as it is reported that CoMgAlO could convert 15.4 % propane with product selectivity of 67.5 % propene, 29.5 % cracking products and 3 % CO_x (Marcu, 2011). This led to investigation of Co content loading, the results where Co_(x)MgAlO mixed oxide catalyst with cobalt content in the range from 1 to 20 % were also reported (Marcu, 2012). Co₍₅₎MgAlO gave the same results as those reported in 2011, and it is worth noting that at Co₍₂₀₎MgAlO the conversion percentage increased to 27% but the disadvantage was that % selectivities gave poor results (Marcu, 2012). The entire results for increasing loading of Co content, is tabulated below;

Table 5: Co_(x)MgAlO catalysts efficiencies with respect to temperature and Co content for Propane conversion to Propene (Marcu, 2012)

Catalyst	Conversion (%)	Selectivity (%)	Temperature
Co ₍₁₎ MgAlO	1.8 – 9.7	96.4 – 70.5	450°C – 600°C
Co ₍₃₎ MgAlO	1.9 – 10.3	96.6 – 70.0	450°C – 600°C
Co ₍₅₎ MgAlO	1.5 – 15.4	92.5 – 67.5	450°C – 600°C
Co ₍₇₎ MgAlO	3.0 – 15.8	92.6 – 52.2	450°C – 600°C
Co ₍₁₀₎ MgAlO	3.1 – 18.0	68.4 – 35.8	450°C – 600°C
Co ₍₂₀₎ MgAlO	6.4 – 27.0	63.4 – 24.1	450°C – 600°C
MgAlO	0.8 – 7.7	10.8 – 25.6	500°C – 600°C

2.4. Concluding Remarks

Dehydrogenation of propane and butane to olefins are great investment opportunity as olefins are building blocks of polymers industry. Current commercialised production of olefins (pyrolysis, catalytic dehydrogenation and steam cracking) suffers lower yields as endothermic nature of the process leads to coke formation.

Oxydehydrogenation has great potential as it is exothermic, thereby eliminating the negative effects of high temperature. However, an introduction of oxygen leads to selectivity issues because the reaction tends to favour CO_x routes (see chapter 3). A very good catalyst is therefore important to overcome this challenge. Many catalysts were reviewed for oxydehydrogenation, and mostly suffer a problem of selectivity. Co₍₅₎MgAlO is the ideal catalyst that is proving to give better selectivity to olefins mainly at lower conversions.

The research conducted will be used to further investigate $\text{Co}_{(5)}\text{MgAlO}$ as catalyst on conversion of butane to olefins, looking closely at how this catalyst behaved when it was used in literature to oxy-dehydrogenate propane.

Chapter 3: Fundamental thermodynamics analysis

3.1. Introduction

Oxy-dehydrogenation has been of research interest since the mid-1980s (Lemonidou, 2005). Many authors have mentioned the thermodynamic benefits of introducing oxygen to alkane's dehydrogenation which lowers the reaction temperature (Grant, 2016) without stating the challenges of selectivity at high paraffins conversions. Cavani (1995) mentioned that the non-catalytic oxy dehydrogenation of propane in quartz reactor, at temperatures from 50 to 100°C higher than that used in catalysed reactions gives an overall yield to olefins higher than any catalysed reaction. All catalysts developed and reviewed in Chapter 2 have shown that as the temperature is increased (following Arrhenius laws) to increase the percentage conversion the selectivity to olefins is negatively affected.

The main aim of this analysis is to draw from fundamentals of thermodynamics to define boundaries at which nature is limiting the oxydehydrogenation of paraffins to olefins, by exploring other possible routes the reaction is taking as temperature is increased.

3.2. Thermodynamic modelling of selectivity

Calculating the reaction Gibbs free energy and enthalpy helps predict the spontaneity of the reaction at certain temperatures (see a picture below), however the exact reaction temperature and reactants conversion percentage towards products is not predicted.

	$\Delta H < 0$	$\Delta H > 0$
$\Delta S > 0$	Spontaneous at all T ($\Delta G < 0$)	Spontaneous at high T (when $T\Delta S$ is large)
$\Delta S < 0$	Spontaneous at low T (when $T\Delta S$ is small)	Non-spontaneous at all T ($\Delta G > 0$)

Figure 5: Gibbs free energy and spontaneity

Looking at Figure 6, the values of Gibbs free energy play an important part of determining the reaction path. Point 1 – 2 where ΔG° is positive favours the reactants and point 4 – 3 where ΔG° is negative the reaction favours products. This information is well defined in literature, what is often not mentioned is the relationship of quotient (product and reaction) versus Gibbs free energy, so that the selectivity can be determined at a particular temperature.

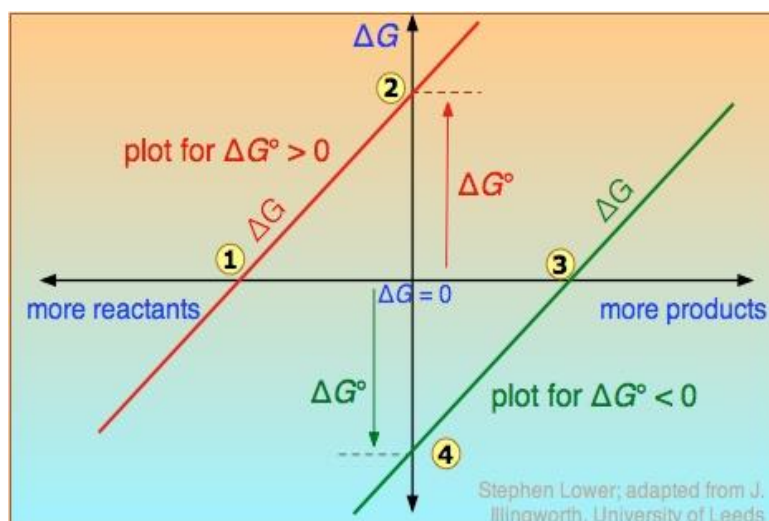


Figure 6: ΔG vs. G° : ΔG is plotted on a vertical axis for two hypothetical reactions having opposite signs of ΔG° ("Lumen learning" n.d).

We are going to use the fundamental concepts of thermodynamics to solve the reaction selectivity vs temperature without catalyst, so that the efficiency of any catalyst can be determined.

From Gibbs free energy equation 3.1 and Enthalpy equation 3.2, Jenkins (2008) derived equation 3.3;

$$G = H - TS \quad 3.1$$

$$H = U + PV \quad 3.2$$

$$dG = VdP - SdT \quad 3.3$$

Substituting ideal gas law, equation 3.4, into equation 3.3 we get equation 3.5;

$$V = \frac{nRT}{P} \quad 3.4$$

$$dG = \frac{nRT}{P} dP - SdT \quad 3.5$$

When we divide by n to change units of energies to kJ/mol and integrate equation 3.5 from point A (formation) to point B (equilibrium) we get equation 3.6;

$$\int_A^B dG = RT \int_A^B \frac{1}{P} dP - \int_A^B SdT \quad 3.6$$

If we assume that entropy does not change with temperature, then equation then becomes;

$$G_b - G_A = RT \ln \frac{P_B}{P_A} \quad 3.6$$

Rearranging equation 3.6 we get equation 3.7

$$\Delta G = \Delta G^\circ + RT \ln Q \quad 3.7$$

Where;

ΔG : Is Gibbs free energy at a temperature T and reaction quotient Q during the reaction

ΔG° : Gibbs free energy of formation at standard temperature and pressure (STP)

R: Universal gas constant

T: Is reaction temperature

Q: is the reaction Quotient of reactants and products

Therefore equation 3.7 can be written like this;

$$\Delta G_b = G_a + RT_b \ln Q \quad 3.8$$

Where;

a : is the initial state STP and;

b : is the state of the reaction at temperature T_b

Figure 6 can now be simplified as below, so that only when Gibbs free energy is negative which is classified with oxy-dehydrogenation reactions.

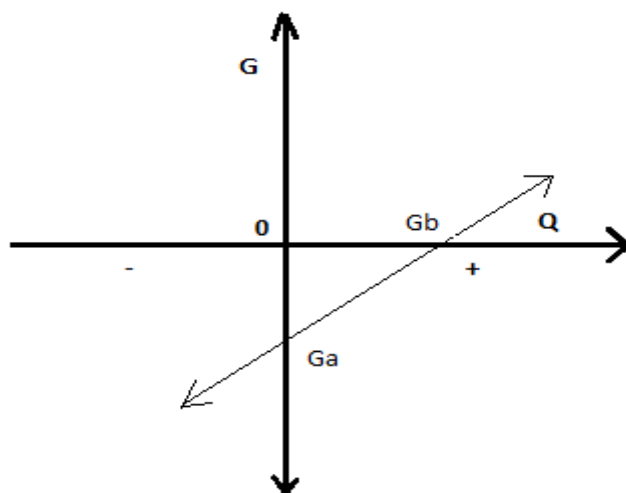


Figure 7: Simplified Oxydehydrogenation Gibbs free energy vs Quotient of the reaction graph

The graph above illustrate that it is always favourable for the value of $\Delta G_a < 0$ because that is when the reaction will move more to the reactants. We are now going to use the information we must determine the temperature T_b and the value of quotient Q for oxy dehydrogenation of propane, so that the selectivity at any temperature can be determined.

3.2.1. Propane oxidative dehydrogenation to propene

Introducing oxygen in the reaction we see the Gibbs free energy of the reaction changing to $\Delta G_a < 0$ thereby favouring the product side.



Calculating ΔG_a we get;

$$= \{(2 \times 74.7) + (2 \times -228.61)\} - \{(2 \times -23.4) + (0)\}$$

$$= -261.02 \text{ kJ/mol}$$

When solving the temperature of the reaction T_b we need to look at Gibbs-Helmholtz equation because we assume that the enthalpy of the reaction does not change as the reaction moves from point a to b (Masuku, 2012) which is;

$$\frac{\Delta G_b}{T_b} - \frac{\Delta G_a}{T_a} \approx \Delta H_a \left(\frac{1}{T_b} - \frac{1}{T_a} \right) \quad 3.10$$

Making ΔG_b the subject of the formula and replacing T_a with 298 K the standard temperature from equation 3.10 above therefore;

$$\Delta G_b = \frac{\Delta G_a T_b}{298} + \Delta H_a - \frac{\Delta H_a T_b}{298} \quad 3.11$$

Substituting 3.11 into 3.7 the equation then becomes;

$$\frac{\Delta G_a T_b}{298} + \Delta H_a - \frac{\Delta H_a T_b}{298} = \Delta G_a + RT_b \ln Q$$

Making T_b the propene (olefin) production temperature subject of the formula, it becomes;

$$T_b = \frac{\Delta G_a - \Delta H_a}{(-R \ln Q) - \left(\frac{\Delta H_a}{298} \right) + \left(\frac{\Delta G_a}{298} \right)} \quad 3.12$$

To solve the temperature ΔT_b value we need to calculate the value of Q and the value (ΔH_a) . ΔH_a ; is calculated below;

$$\Delta H_a = \sum Products - \sum Reactants \quad 3.13$$

$$= \{(2 \times 20.2) + (2 \times -242)\} - \{(2 \times -104.5) + (0)\}$$

$$= -234.6 \text{ kJ/mol}$$

To get the quotient of products and reactant, Q , we use the mass law action, which states that the values of equilibrium constants which can be expressed as K_p are constant for any reaction at a particular temperature (T_b), whenever equilibrium concentrations are substituted into the equation 3.7 below (Gammon, 2002).

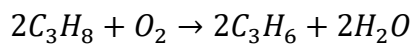
Now if we assume that the equilibrium is reached at each temperature (T_b) for a reaction of gases A and B below to give product C and D with coefficient a, b, c and d to balance the chemical reaction then the expression of the reaction would be written as follows;



Therefore, calculating the quotient Q or equilibrium constant K_p at temperature T_p then we get equation 3.15 below:

$$K_p = \frac{[C]^c[D]^d}{[A]^a[B]^b} \quad 3.15$$

Now considering the route of formation of olefins from oxy dehydrogenation of paraffins equation 3.3 will come in effect;



If we start with 2 moles of Paraffin and 1 mole of Oxygen, and the products are 2 moles of propene and 2 moles of water. The reaction moles distribution for x moles of oxygen reacted, will be as follows from beginning to the end of the reaction.

$$\text{Start : } 2 + 1 \rightarrow 0 + 0$$

$$\text{during : } (2 - 2x) + (1 - x) \rightarrow 2x + 2x$$

$$\text{End: } 2 - 2x + 1 - x + 2x + 2x$$

$$\text{Total number of moles at end of reaction: } 3 + x$$

We know that Q can be replaced with K_p at equilibrium

$$K_p = \frac{[Product]}{[Reactants]} = \frac{[C_3H_6]^2 \cdot [H_2O]^2}{[C_3H_8]^2 \cdot [O_2]} \quad 3.16$$

To find the concentrations of products and reactants we need to apply Dalton's law of partial pressures which is;

$$P_i = y_i P_{Tot}$$

3.17

Where P_i = partial pressure of a single gas

y_i = fraction of partial pressure of gas in total number partial pressures of all gases

P_{Tot} = total pressure of all gases

Therefore; $y_{olefins; H_2O} = \frac{2x}{3+x}$ and;

$y_{O_2} = \frac{1-x}{3+x}$ lastly;

$y_{paraffins} = \frac{2-2x}{3+x}$

Substituting these fractions in equation 3.16 we get;

$$K_p = \frac{\left(\frac{2x}{3+x}\right)^2 \left(\frac{2x}{3+x}\right)^2}{\left(\frac{2-2x}{3+x}\right)^2 \left(\frac{1-x}{3+x}\right)}$$

Simplifying the fraction, we get;

$$K_p = \frac{16x^4}{(3+x)(2-2x)^2(1-x)} \quad 3.18$$

If the percentage conversions run from 0% to 100%; x values can be varied between the fractions 0 – 1 to get the values of K_p (see table below).

Table 6: Table of % conversions (x) and Value of K_p

x	K_p
0.1	0
0.2	0.000177
0.3	0.003906

0.4	0.028624
0.5	0.139434
0.6	0.571429
0.7	2.25
0.8	9.613614
0.9	53.89474
1	Undefined

Substituting gas constant $R = 0.00831 \text{ kJ/mol.K}$ and K_p into equation 3.12 the values of the reaction temperature T_b at given % conversion x can be determined.

3.2.2. Propane oxidative dehydrogenation to other routes

There are other routes in addition to propene that the reaction of propane oxidation can take; below we did similar work with that done in 3.2.1. (See appendix). The summary of K_p fractions as well as enthalpy and Gibbs free energies are tabulated.

The reactions routes are;

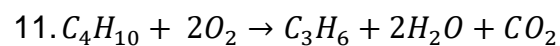
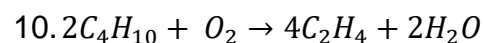
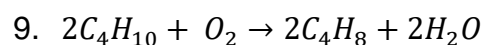
1. $C_3H_8 + 5O_2 \rightarrow 3CO_2 + 4H_2O$
2. $2C_3H_8 + 7O_2 \rightarrow 6CO + 8H_2O$
3. $C_3H_8 + O_2 \rightarrow 2CH_4 + CO_2$
4. $2C_3H_8 + O_2 \rightarrow 4CH_4 + 2CO$
5. $C_3H_8 + O_2 \rightarrow C_3H_5OH + H_2O$
6. $C_3H_8 + O_2 \rightarrow C_3H_4 + 2H_2O$
7. $2C_3H_8 + 3O_2 \rightarrow 2C_2H_4 + 4H_2O + 2CO$
8. $C_3H_8 + O_2 \rightarrow C_2H_6 + H_2 + CO_2$

Table 7: Table of reaction (1 – 8) H_a and G_a with K_p

<i>Products</i>	<i>H_a kJ/mol</i>	<i>G_a kJ/mol</i>	<i>K_p</i>
(1) $3CO_2 + 4H_2O$	−2044	−2074.21	$\frac{6912x^7}{(6+x)(1-x)(5-5x)^5}$
(2) $6CO + 8H_2O$	−4088	−2605.46	$\frac{7.83 \times 10^{11}x^{14}}{(9+5x)^5(2-2x)^2(7-7x)^7}$
(3) $2CH_4 + CO_2$	−438.74	−472.59	$\frac{4x^3}{(2+x)(1-x)^2}$
(4) $4CH_4 + 2CO$	−311.48	−430.86	$\frac{1024x^6}{(3+3x)^3(2-2x)^2(1-x)}$
(5) $C_3H_5OH + H_2O$	−372.8	−367.71	$\frac{x^2}{(1-x)^2}$
(6) $C_3H_4 + 2H_2O$	−194.1	−239.22	$\frac{4x^3}{(2+x)(1-x)^2}$
(7) $2C_2H_4 + 4H_2O + 2CO$	−875.2	−1005.9	$\frac{4096x^8}{(5+3x)^3(2-2x)^2(3-3x)^3}$
(8) $C_2H_6 + H_2 + CO_2$	−374	−403.99	$\frac{x^3}{(2+x)(1-x)^2}$

3.2.3. Butane oxidative dehydrogenation to other olefins

For Butane we are only going to look at olefins products when paraffin reacts with oxygen. The following reactions are noted below as the possible routes for reactions,



Similar steps of calculating (K_p), G_a and H_a as those in propane oxydehydrogenation were followed and the results are tabulated below;

Table 8: Table of reaction (9 – 11) H_a and G_a with K_p

<i>Products</i>	<i>H_a kJ/mol</i>	<i>G_a kJ/mol</i>	<i>K_p</i>
(9) $2C_4H_8 + 2H_2O$	-229.8	-280.62	$\frac{16x^4}{(3+x)(2-2x)^2(1-x)}$
(10) $4C_2H_4 + 2H_2O$	-20.4	-150.82	$\frac{1024x^6}{(3+3x)^3(2-2x)^2(1-x)}$
(11) $C_3H_6 + 2H_2O + CO_2$	-602.9	-742.91	$\frac{4x^4}{(3+x)^1(2-2x)^2(1-x)}$

3.3. Results and Discussions

3.3.1. Propane oxy-dehydrogenation routes

Table 9 and Figure 8 below illustrate the relationship of selectivity to propene at all equilibrium points relative to temperature (T_b).

Table 9: Temperature T_b of reaction for % conversion x of propane to propene

x	K_p	T_b (K)	T_b (°C)
0	0		
0.1	0.000177	1566.597	1293.597
0.2	0.003906	620.5185	347.5185
0.3	0.028624	446.8259	173.8259
0.4	0.139434	365.4945	92.4945
0.5	0.571429	314.4964	41.49644
0.6	2.25	276.9492	3.949224
0.7	9.613614	245.8481	-27.1519
0.8	53.89474	216.9309	-56.0691
0.9	672.9231	185.0537	-87.9463
1			

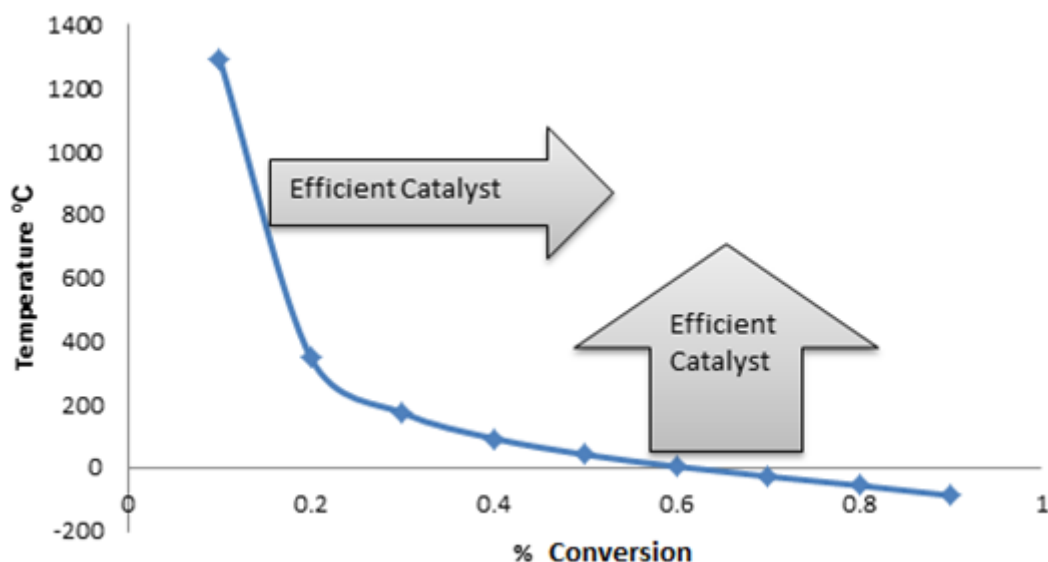


Figure 8: Relationship between Temperature (T_b) versus propane conversion %

From the graph above it is evident that for a good catalyst to be deemed efficient it should be able to give high conversion percentage of above 30% at moderate temperatures of below 200°C for olefin selectivity. If the catalyst discussed in Chapter 2 are plotted on the graph above for oxy dehydrogenation of propane to propene, the graph then looks like this;

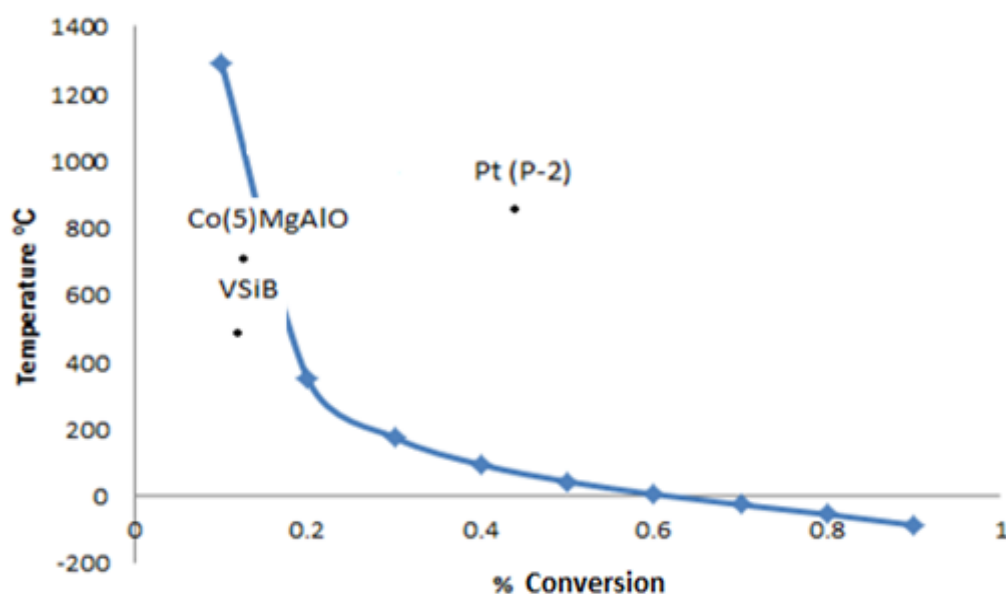


Figure 9: Relationship between Temperature (T_b) versus propane conversion % with catalysts plots.

The results for propene selectivity reduction as the propane conversion increases tally with that reported by (Kung, 1997) for Vanadium catalysts.

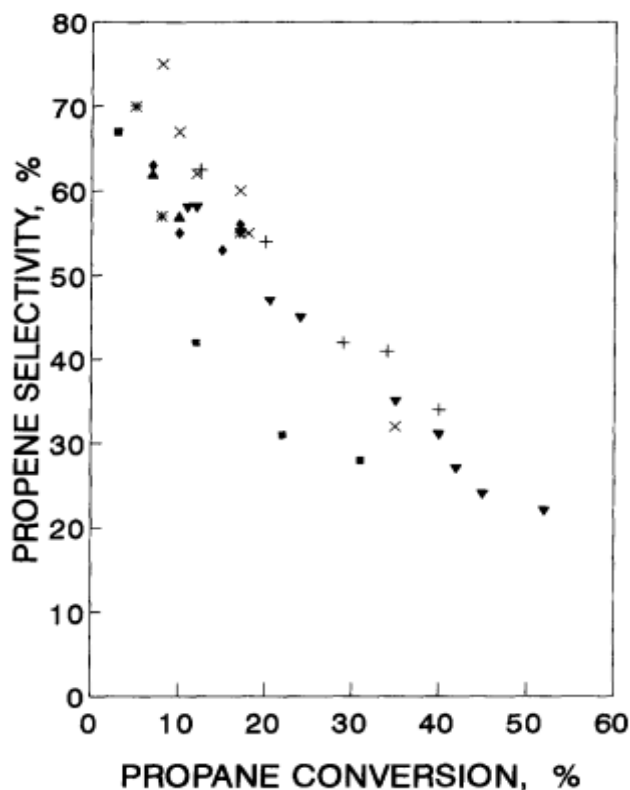


Figure 10. Relationship between propane conversion and propene selectivity (Kung, 1997)

When it is put against other catalysts; Co_5MgAlO has proven to be a better catalyst with lower reaction temperatures and higher conversion %. With $\text{VSi}\beta$ the catalyst does not follow the theoretical calculations as it gives higher conversion at low selectivity; it is even difficult to put the point on the figure 9 above.

The challenge with oxidative dehydrogenation must be the other routes the reaction takes around these temperature(s), in when the stoichiometric ratio of hydrocarbons and oxygen is slightly changed. Theoretical changes where other olefins and alcohols are produced are as follows;

Table 10: % conversion and reaction temperatures for olefins and alcohol routes

Temperature (T_b) °C for olefins and alcohol routes				
x	C3H4OH	C3H4	C2H4	C3H6
0	-	-	-	-
0.1	-178.0344953	168.4823981	195.1235232	1293.5968
0.2	-146.1329773	100.9931086	124.5042908	347.5185392
0.3	-109.6633229	67.93213059	90.05148021	173.8258705
0.4	-59.30834321	45.8239647	67.10095702	92.49450087
0.5	25	28.6138771	49.29453283	41.49643739
0.6	219.181812	13.7465307	33.95365119	3.949223988
0.7	-	-0.342157671	19.44474826	-27.15193234
0.8	-	-15.22468128	4.133102946	-56.06914788
0.9	-	-34.13607934	-15.33830635	-87.94630366
1	-	-	-	-

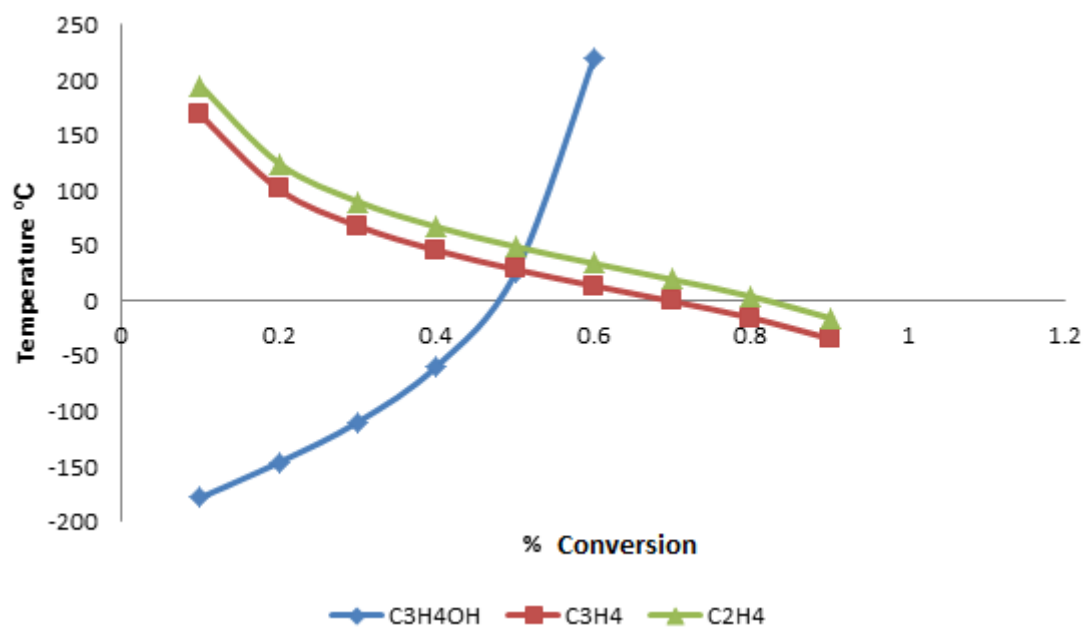


Figure 11: Relationship between Temperature (T_b) versus other hydrocarbon's conversion %

The information above illustrate that even though other reactions which are beneficial to overall olefins productions are possibly selected when the stoichiometric ratios are

changed, these olefins productions are also at very low conversions as compared to alcohols.

Furthermore the statement made by (Kung, 1992) stating that the easier it is to reduce the oxide on the surface of catalyst, the more likely it will be attach to the hydrocarbon intermediates attacking C-C and C-H bonds with same intensity to results in carbon oxides. Most of the selectivity is shared with other undesired routes – carbon oxides and short hydrocarbons – and these different routes where also tabulated with their conversion % at selectivity lines of each product and the reaction temperature (T_b). The table 11 and figure 11elow illustrate these;

Table 11: % conversion and reaction temperatures for undesired routes

x	Temperature (T_b) °C for undesired routes				
	CO ₂ + H ₂ O	CO + H ₂ O	CH ₄ +CO ₂	CH ₄ + CO	C ₂ H ₆
0	-	-	-	-	-
0.1	-	10.99502462	252.7653105	118.7441554	499.545302
0.2	-	15.72150045	135.6923253	78.04829947	247.019972
0.3	474.2863597	18.78759989	85.10910979	57.1281678	157.711313
0.4	193.8101245	21.22831229	53.41824859	42.85652031	106.575893
0.5	75.61261528	23.40159452	29.83660755	31.61258469	70.6731122
0.6	6.043982162	25.51203852	10.1860611	21.80021203	42.0502864
0.7	-43.1758232	27.74954924	-7.849479797	12.39413579	16.7534616
0.8	-83.36877859	30.41395483	-26.31109809	2.297561021	-8.2281683
0.9	-122.4015328	34.35240583	-48.93965114	-10.88261539	-37.6591018
1	-	-	-	-	-

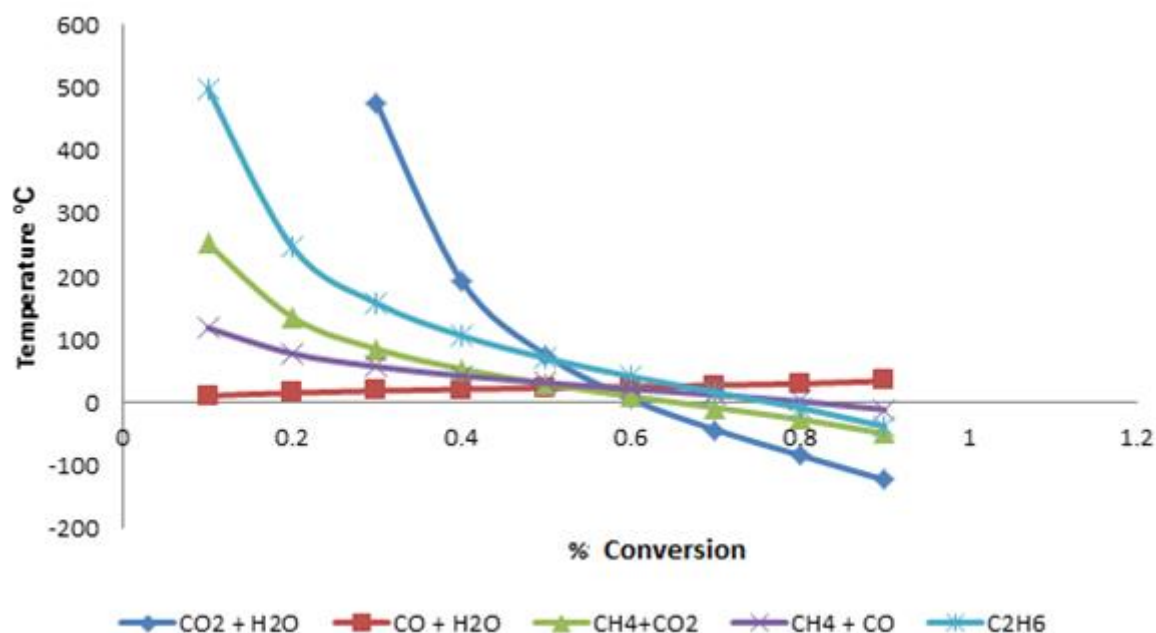


Figure 12: Relationship between Temperature (T_b) versus undesired routes conversion %

We then did literature analysis of our plots to see how far they are from know data. We reviewed our plots using (Kung, 1992) experimental data where he was doing oxidative dehydrogenation of propane, and table 12 below shows his results.

Table 12: Product selectivities and conversions for Mg orthovanadate and Mg pyrovanadate (Kung, 1992)

Catalyst	Temp. (°C)	Feed O ₂ /HC/He	Conv. (%)	Product selectivities (%)			
				CO	CO ₂	Alkenes	1,3-butadiene
<i>Oxidation of propane</i>							
Mg ₃ (VO ₄) ₂	541	10/1/39	6.7	10.1	26.3	63.6	
Mg ₂ V ₂ O ₇	502	11/1/88	7.9	20.9	17.7	61.4	
	510	2/1/22	12.0	27.2	18.4	54.4	

^a Catalysts were prepared as described in ref. [2], using Mg(NO₃)₂ and (NH₄)₂CO₃ as precursors.

(Kung, 1992) experimental results when compared to our computed thermodynamic plots give slight similarities especially when it comes to carbon oxides compositions at low % conversions and temperature around 500°C.

3.3.2. Butane oxy dehydrogenation to butylene and other hydrocarbons

Butane oxy-dehydrogenation has a potential to produce butylene and other hydrocarbons, as well undesired side reactions as with propane oxy-dehydrogenation. The results on Butane oxy dehydrogenation will however focus on the production of butylene and other useful hydrocarbons. The results for temperature and % conversion is tabulated below, with a graph to show the relationship between the two variables following;

Table 13: Percentage selectivity and reaction temperatures for olefins routes

	Temperature (T_b) °C for undesired routes		
x	C4H8	C2H4	C3H6
0	-	-	-
0.1	233.6857065	106.2787668	87.54981752
0.2	132.0867154	71.63858828	65.61425085
0.3	85.77921237	53.45105353	52.85341267
0.4	55.89062626	40.89144408	43.37519014
0.5	33.16811933	30.90802708	35.38394297
0.6	13.90828452	22.13129707	27.99676283
0.7	-4.020836017	13.66104178	20.54583074
0.8	-22.59533388	4.506320817	12.16656149
0.9	-45.59351142	-7.543117514	0.723697026
1	-	-	-

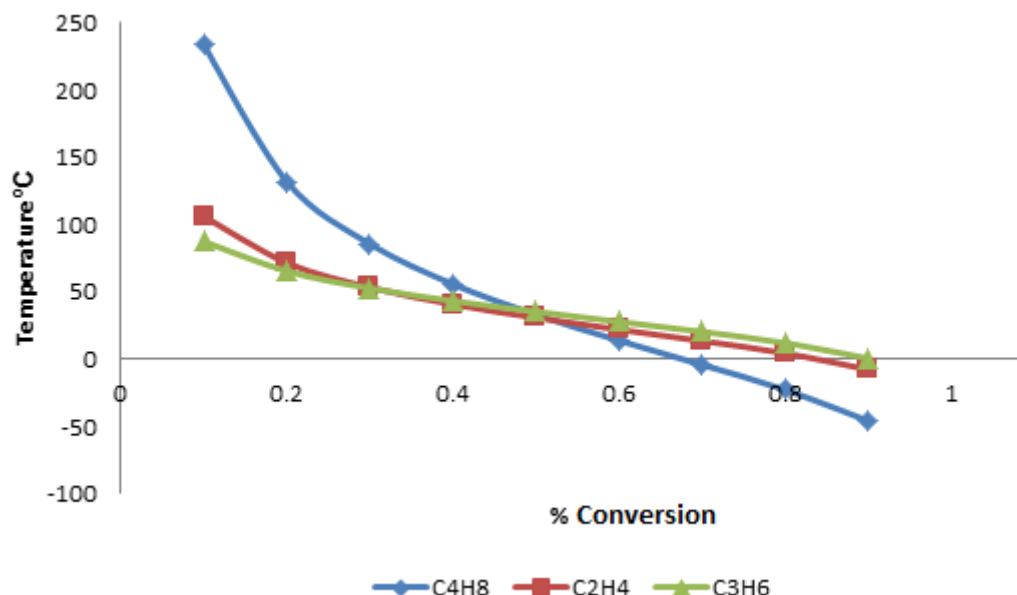


Figure 13: Relationship between Temperature (T_b) versus olefins routes selectivity %

3.4. Concluding Remarks

Even though some chemical innovations have been found by chance, it is always costly when experimental work is done by trial and error. Most chemical reactions are heat sensitive; therefore, it is wise to study reactions thermodynamic limits to understand temperature ranges available in nature before conducting any experimental work.

This thermodynamic study has shown that oxidative dehydrogenation of propane and butane even though able to lower the reaction temperatures, suffers the problem of selectivity. $\text{Co}_{(5)}\text{MgAlO}$ has proved to be a good catalyst for oxy-dehydrogenation of propane to propene as it was able to give better results, than other literature catalyst when it comes to selectivity at lower temperatures.

The extension of this research will be to try and see how this catalyst would behave when it is experimented with butane for oxy dehydrogenation to produce olefins. The Chapters that follow will address this very issue of seeing how $\text{Co}_{(5)}\text{MgAlO}$ behaves during oxy-dehydrogenation of butane to olefins.

Chapter 4: Experimental Details

4.1. Introduction

This chapter outlines the materials used, catalytic preparation and experimental measurements procedures used in the dissertation.

4.2. Materials used

The materials used in our experiment are as follows: Cobalt (II) nitrate hexahydrate (Sigma – Aldrich, $\geq 98\%$), Aluminium nitrate nonahydrate (Sigma – Aldrich, $\geq 98\%$), Magnesium nitrate hexahydrate (Sigma – Aldrich, $\geq 98\%$), Sodium hydroxide pellets (low chloride) (Merck, $\geq 97\%$), quartz-wool, Ethane, Butane, Propane and Oxygen cylinders. Cylinders were supplied by African Oxygen (AFROX Ltd).

4.3. Catalytic preparation

Co/Mg/Al LDHs precursor was produced by co-precipitation of different metal nitrate solutions using an aqueous solution of NaOH and Na_2CO_3 as maintainer of pH between 9 and 10 under room temperature. An aqueous solution containing a mixture of 13 ml distilled water, 4.4 g of $\text{Mg}(\text{NO}_3)_2 \cdot 6\text{H}_2\text{O}$ and 2.1 g of $\text{Al}(\text{NO}_3)_3 \cdot 9\text{H}_2\text{O}$ was labelled sample A. A solution containing 36g of NaOH (2M) and 14.4g of Na_2CO_3 (1M) was added into 450 ml of distilled water and was labelled sample B. Sample C contained an aqueous solution 5g of $\text{Co}(\text{NO}_3)_2 \cdot 6\text{H}_2\text{O}$ in 13 ml distilled water. The cobalt content as a molar percentage with respect to cations was maintained at 5% ($\text{Co}/(\text{Co}+\text{Mg}+\text{Al})=0.05$), with molar ratio of $\text{Mg}/\text{Al} = 3$. Therefore extra 0.58g of Co^{2+} was added to the $\text{Co}(\text{NO}_3)_2 \cdot 6\text{H}_2\text{O}$ solution.

Sample A and B where added by drop wise addition into a well stirred sample C while maintaining $9 \leq \text{pH} \leq 10$. The precipitate formed was then matured in the mother liquor

overnight at 80 °C under stirring, separated by centrifugation, washed with deionised water and then dried at 80 °C overnight.

The dried LDH sample was then after noted as Co₍₅₎MgAl – LDH, the LDH precursor was then calcined in air at 750 °C for 8 hours in order to obtain the required catalyst which is Co₍₅₎MgAlO.

4.4. Characterization

4.4.1. Bulk characterisation: XRD measurements

The following settings were used on XRD to run sample:

Generator settings had a tension of 40 and voltage was 40kV with configuration of spinner reflection. Measurement type was an absolute scan and 2 Theta with a range from 5 degree to 80 degree. Step size - 0.0167; Time per step: 15.240s; Scan speed: 0.139 degree/seconds with number of steps: 4488 where used. Divergence slit was fixed at slit 1 degree with anti-scatter slit: fixed slit 2 degree

4.4.2. Surface characterisation

4.4.2.1. TGA measurements

TGA samples were obtained using model simultaneous thermal analyser (STA) 1500 (Rheometric Scientific Ltd UK), over nitrogen at heating rate of 10 °C/min from 50 °C to 1000 °C.

4.4.2.2. BET measurements

BET surface area measurements were conducted Micromeritics Tri-Star to determine any loss of surface area after loading the metal. The catalyst sample was slowly heated to 706 °C and held at this temperature for 4 hours under vacuum (~7 kPa). A dry sample was cleaned of all contaminated gases and cooled to -198 °C using liquid nitrogen.

4.4.2.3. TPR measurements

The sample was heated under flowing helium (30ml/min) from room temperature to 120 °C and held at this temperature for 30min (ramp rate= 10 °C/min); to remove moisture and possible contaminants.

The sample was then cooled to 50 °C under flowing helium and held at this temperature for 5min. The gas flow was changed to 10%hydrogen in argon (30ml/min) and the sample temperature was then ramped to 950 °C at a rate of 10 °C/min and the hydrogen consumption was monitored (TCD signal)

4.5. Experimental Conditions

For the ODH experiments, mild operating conditions were preferred, which are atmospheric pressure (1atm) and temperature of 350 °C or less. The process conditions were chosen to reduce the capital cost of possible application of this experiment on industrial level.

Before each experiment the catalyst was activated under air at 350 °C.

Series of runs are then conducted with flow rates of paraffins at 10 mL/min for Propane and Butane. The oxygen (air) volumetric flowrate was then varied between 0 mL/min – 57 mL/min across paraffins. Oxygen (air) volumetric flowrates were calculated to maintaining the stoichiometric non combustion conditions of hydrocarbons and Oxygen. The aim was to test the selectivity and yields of olefins at different oxygen volumetric flowrates over propane and butane.

The steps that were involved in the Oxidative dehydrogenation of light paraffins experiments were: 1. Rig building, 2. loading of catalyst, 3. Performing ODH reactions at different oxygen (air) volumetric flowrates.

4.6. ODH Reactors

A brief description of the reactor system and specification is outlined below. A fixed bed reactor was used in this study. **Figure 14** shows the dismantled reactor with fittings. The materials used for the reactor is stainless steel with tube length of 204 mm and internal diameter of 8 mm, with screwed end fittings (Gorimbo, 2016).



Fig 14: Dismantled reactor photograph. (Gorimbo, 2016)

4.7. Catalyst loading into the reactor

Before the catalyst was loaded, the ODH rig was tested with nitrogen gas for any leaks. After the fitting joints and lines were determined to be tight, the reactor was detached from the rig. Figure 15 illustrates the schematic representation of ODH reactor with quartz chips, Cobalt catalyst and a thin layer of quartz wool (Gorimbo, 2016). The middle part of the reactor was measured and stuffed with soft quartz wool and 1 gram of catalyst placed in catalyst bed. Then the quartz chips were added at the top and bottom of the middle part of the reactor to fill the empty space to avoid potential gas phase reactions at high temperatures.

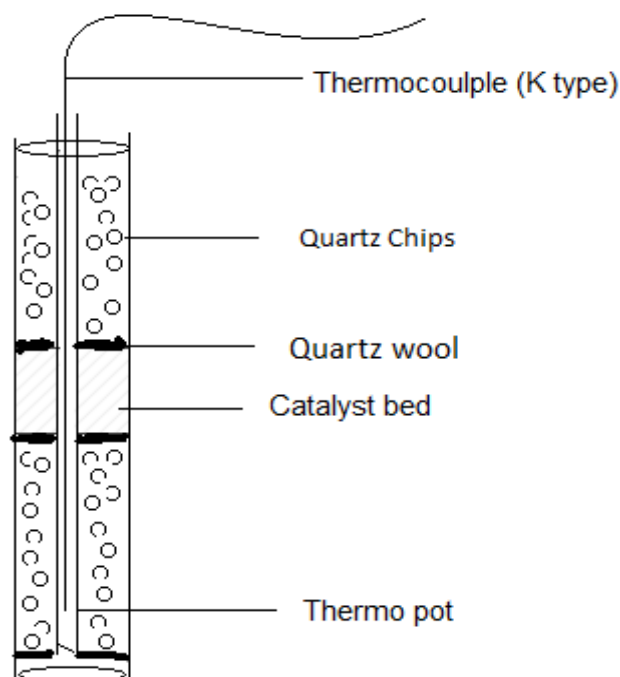


Figure 15: ODH reactor with loaded catalyst (Gorimbo, 2016)

After loading catalyst, the leakage testing was performed once more to see if there was no leakage. The reactor was insulated with thermal jacket to prevent heat loss. The top, middle and bottom part of the reactor was heated with heating coils forming a heating element. Temperature controllers were used to enable the setting to the desired temperatures.

4.8. Experimental set-up

Figure 16 illustrates the experimental set-up which was built to achieve the aim of the study. The feed of paraffins and oxygen was controlled by Brooks mass flow controllers (Brooks Instrument 5850). Each mass flow controller was mounted with non-return valve to ensure that no product was flowing back into the mass flow controller. Back pressure regulators were used manually to control the pressure inside the reactors. All the experiments were conducted under the laboratory scale fixed bed reactor set-up as shown below;

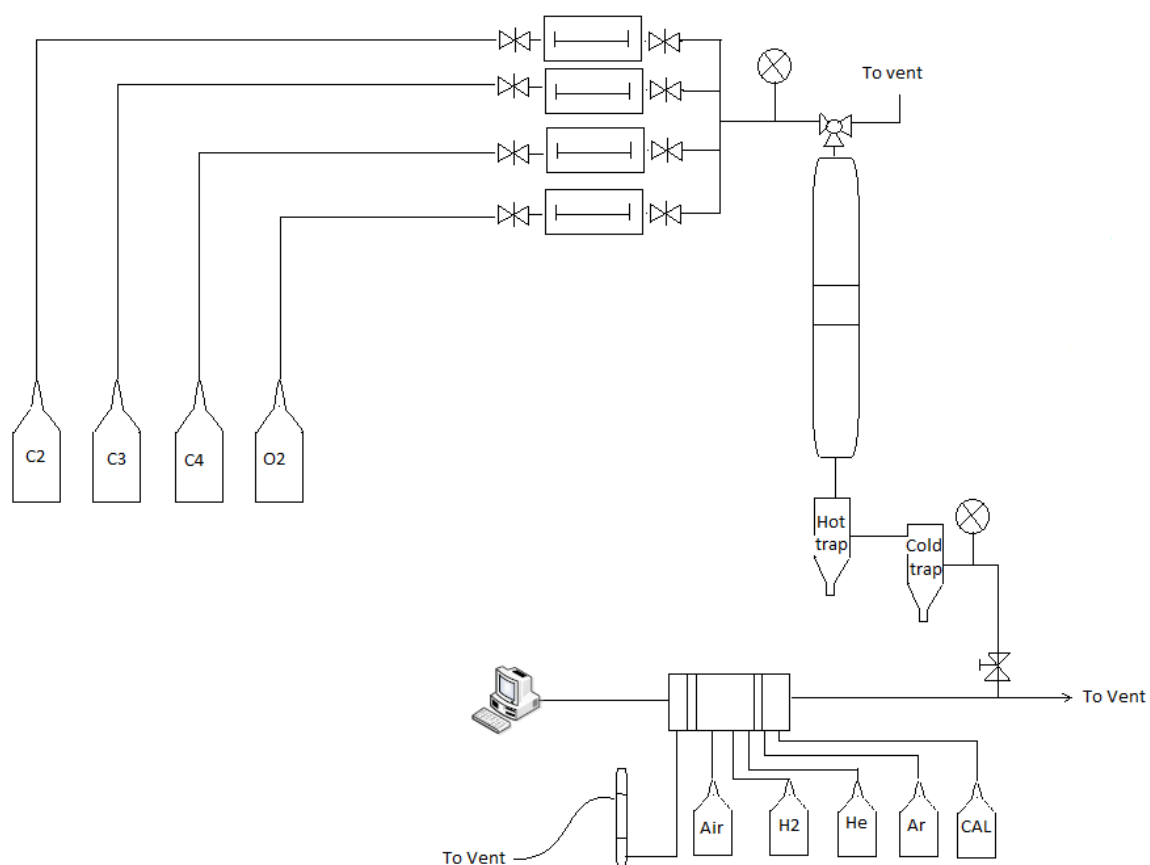
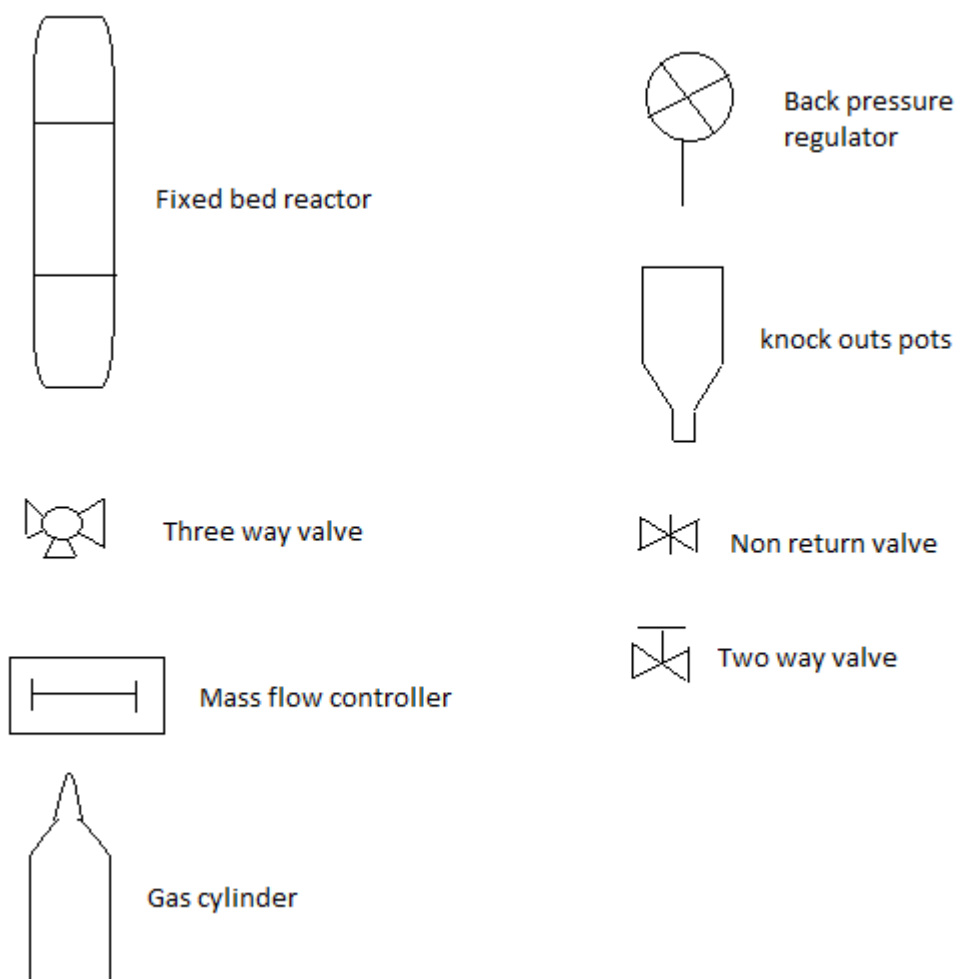


Figure 16: Laboratory scale ODH rig flow scheme of fixed reactor



4.9. Experimental method

4.9.1. Catalyst activation procedure

Before catalyst cleaning, one gram of a catalyst in the reactor was dried with nitrogen at 60 mL/min, at temperature of 120 °C, and at atmospheric pressure for 2 hours, to remove any unwanted moisture accumulated during loading. Temperature increase was achieved by increasing from room temperature of approximately 27 °C to 70 °C at a heating rate of 5°C/min then held for 20 min at 70 °C. Temperature was then increased to 120 °C at heating rate of 2 °C, overnight.

Air was then passed onto catalyst at the flow rate of 60 mL/min, at temperature of 350 °C, and at atmospheric pressure, for 2 hours to clean the surface of the catalyst for any unwanted materials accumulated during loading. The temperature was increased from drying of 120 °C to 350 °C the cleaning temperature at the heating rate of 2°C/min. The system was then left at 350 °C for 1 hour before the ODH reaction could be conducted.

4.9.2. ODH reaction runs

After the catalyst activation, paraffin (Butane) gas was passed into the reactor at the flow rate of 10 mL/min. The temperature was maintained at 350 °C and the system was at atmospheric pressure. Air was not administered for run 1 and the system was left to settle for 3 hours before the results could be taken. For run 2 to 4 air volumetric flow rate was then increased gradually until 57 mL/min.

Propane and butane has similar stoichiometric ratio. The flow rate of the hydrocarbon (Propane and Butane) was also maintained at 10 mL/min for run 1 – 4 while the flow rate of air was increased from 0 mL/min at run 1 up to 57 mL/min at run 4. **Table 14** below shows a summary of reaction flow rates of paraffins and oxygen for each run.

Table 14: Reaction flow rates for Paraffins and Oxygen for run 1 – 4.

Run	Butane Flowrate (mL/min)	Butane : O ₂ ratio	O ₂ run(mL/min)	Air run(mL/min)
1	10	1 : 0	0	0
2	10	1 : 0.4	4	19
3	10	1 : 0.8	8	38
4	10	1 : 1.2	12	57

Chapter 5: Results and Discussions

5.1. Catalytic Characterisation

5.1.1. XRD

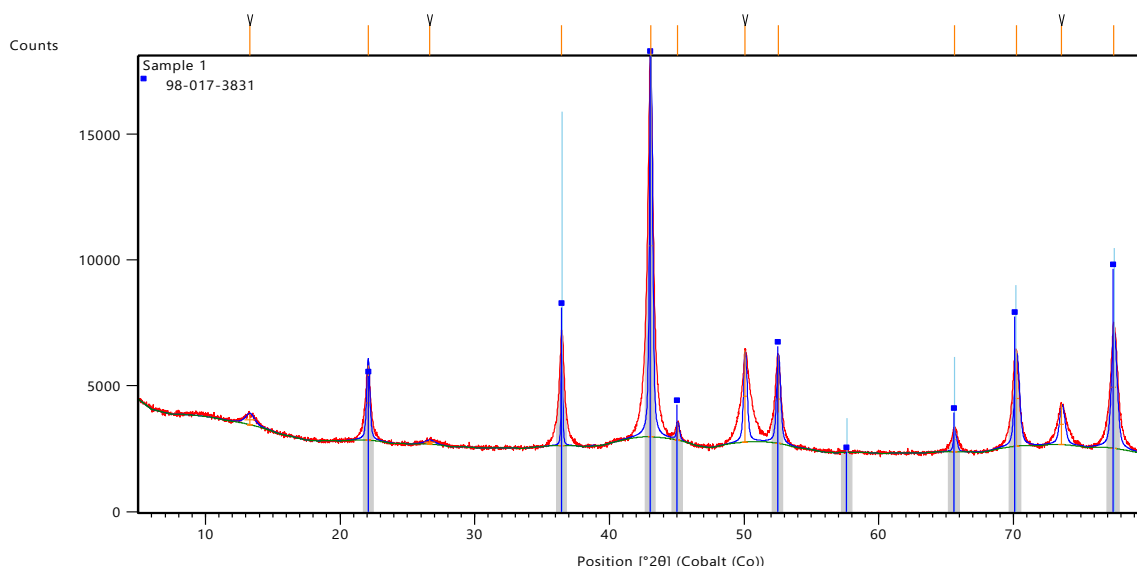


Figure 17: XRD patterns of Co_5MgAlO

The XRD pattern of Co_5MgAlO samples calcined at 750°C is displayed in fig. 17 above. From the figure it can be seen that the sample exhibited the reflections at 2θ values $\sim 37.5^\circ$, 43.5° and 63° characteristic of a well-known $\text{Mg}(\text{Al})\text{O}$ periclase-like phase as reported by Marcu (2012). Peaks that are consistent with Co-related phase (Co_3O_4 and/or CoAl_2O_4), characterised by diffraction peaks $\sim 22.1^\circ$, 36.6° , 43.1° , 52.7° , 65.7° , 70.3° and 77.6° as noted by Meng (2009) were also visualised in this case. Mg – related peaks are detected in the periclase-like phase. It was noticed after the calcination that the catalyst displayed a light blue colour, suggesting the presence of CoAl_2O_4 or CoAl_2O_4 –like spinel phases (Meng, 2009). This is noted as difference between our catalyst and the reference catalyst. The reference catalyst didn't display Co-containing phases, these could be because it was well dispersed in the MgAlO matrix.

5.1.2. TGA

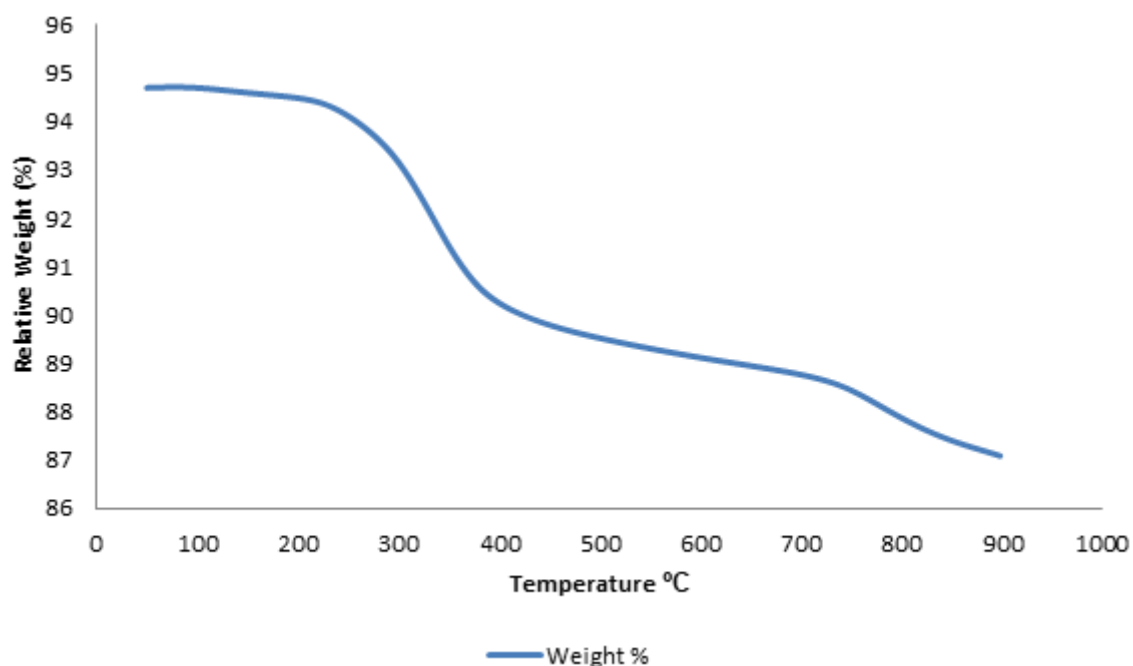


Figure 18: The TGA profile for the Co₅MgAlO catalyst

The TGA profile is shown in figure 18 above, three stages corresponding to the weight % loss peaks are associated with the thermal degradation of the of the hydrotalcite compounds (Li, 2009). Initial stage between 100 °C and 200 °C is attributed to the loss of the intermolecular layer and water molecules absorbed while the layered structure is maintained. Hydroxyl water and the inter-layer nitrate anions are removed around 350 °C and at this stage part of the layered structure are collapsed. Upon heating at around 750 °C, complete pyrolysis occurs, and the layered structure is completely destroyed.

5.1.3. H_2 consumption – TPR

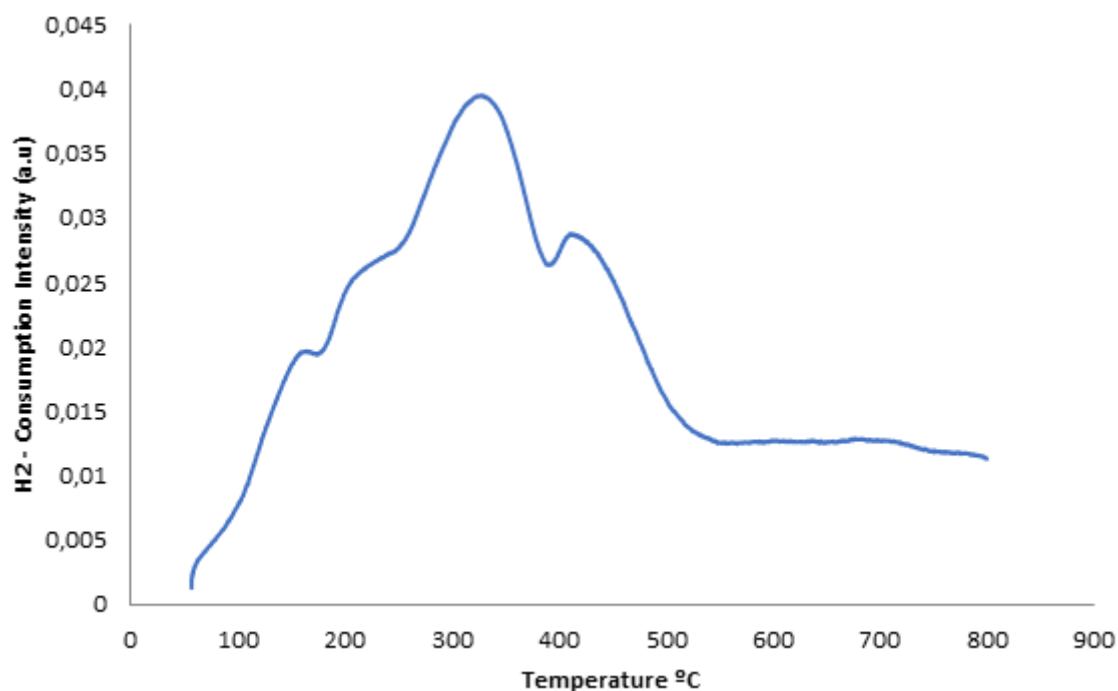


Figure 19: H_2 – TPR profiles of Co_5MgAlO catalyst

For the investigation of redox properties of Co_5MgAlO catalyst, the H_2 consumption – TPR measurement was performed. The results are illustrated in Fig 19 above. The profile of the catalyst shows two reduction regions, the first one between 250 °C and 470 °C and second one above 500 °C. The first one can be due to the reduction of Co^{3+} to Co^{2+} dispersed in the Co_3O_4 phase (Meng, 2009), while the second one should be attributed to the reduction of both surface Co^{2+} ions and subsurface Co^{2+} in dilution with Co^{2+} - Al^{3+} spinel or stoichiometric $CoAl_2O_4$ (Li, 2009). There is a correlation of these findings with those found in XRD results which suggested the coexistence of Co_3O_4 and $CoAl_2O_4$ in view of the high Co content in the sample.

5.1.4. Textural analysis

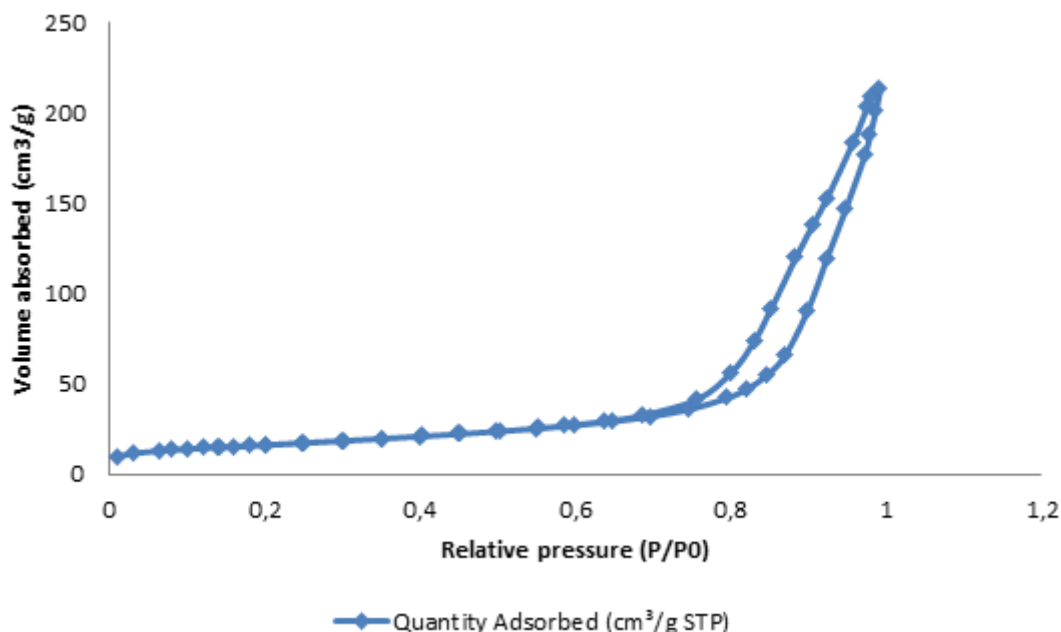


Figure 20: Nitrogen adsorption/desorption isotherms profile at -195 °C Co₅MgAlO catalyst

The catalyst displayed type IV nitrogen adsorption/desorption isotherms, which is in accordance with the IUPAC classification, and H3 – type hysteresis loops which are characteristic of mesoporous materials (Marcu, 2012). It is also noted that the absorption isotherms do not present plateau at high P/P_0 values showing N₂ physisorption was taking place between the aggregates of platelets particles and accounted for the lamellar morphology of the materials (Marcu, 2012).

5.2. Oxidative dehydrogenation reactions

5.2.1. Butane oxy dehydrogenation

Table 15: Conversion % of Olefins and Oxygen and Product selectivity % for Oxidative dehydrogenation reaction

	Ratio of Butane to Oxygen		
	Run 1 1:0.4	Run 2 1:0.8	Run 3 1:1.2
<i>Conversion</i>	%	%	%
C ₄ H ₁₀	-	11.92	26.16
O ₂	-	99.74	99.74
<i>Product selectivity</i>	%	%	%
C ₂ H ₄	-	1.58	2.43
C ₂ H ₆	-	0.59	0.71
CO ₂	-	85.18	84.67
1-C ₄ H ₈	-	12.65	12.19

At 350°C and atmospheric pressure a reaction product of 1:0.4 ratio of butane to oxygen gave inconclusive results. Butane to oxygen ratio of 1:0.8 had an olefin production decreased to less than 14% combined olefins production. Increased the oxygen even further at 1:1.2 similar product composition was realised.

Figure 22 below tells us that it is thermodynamically impossible to get to high selectivity %, at moderate temperatures $\geq 50^\circ\text{C}$ by pushing the reaction conversions to more than 40%. Our experimental data also proved to correlates with the thermodynamic plots we have computed in chapter 3.

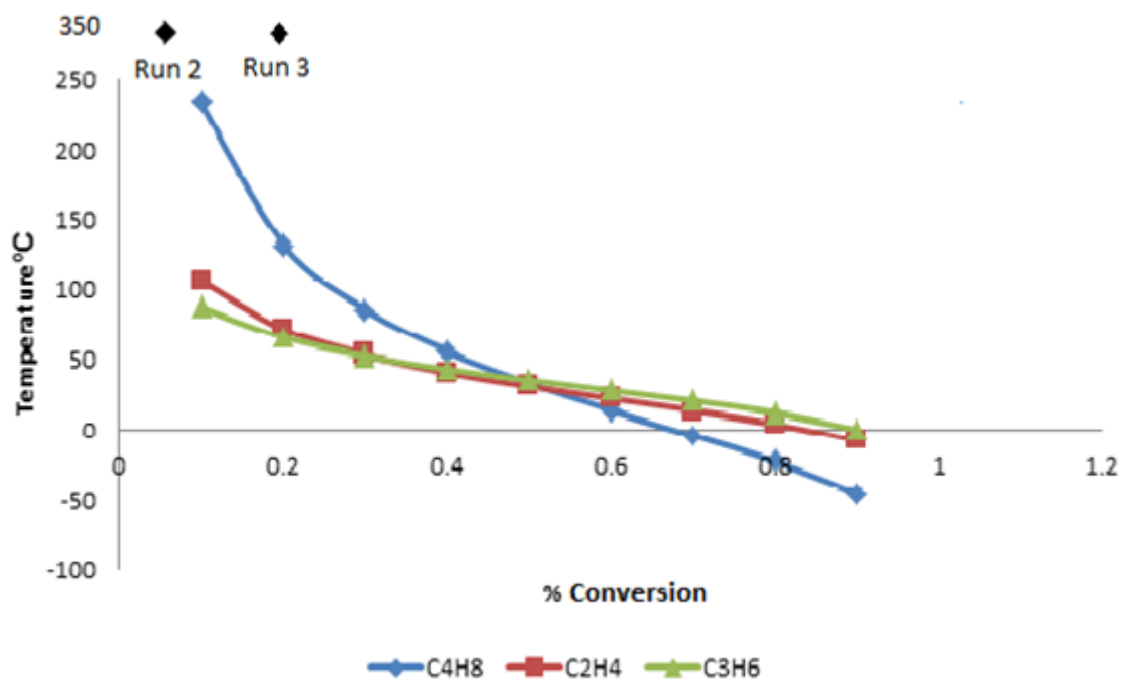


Figure 22: Reaction runs on thermodynamic plots for olefin cut.

(Kung, 1992) did experimental work where he was investigating the effect of Mg Orthovanadate and Mg Pyrovanadate at temperatures higher than 500°C. Table 17 below shows his results.

Table 16: Product selectivities and conversions for Mg orthovanadate and Mg pyrovanadate (Kung, 1992)

Catalyst	Temp. (°C)	Feed O ₂ /HC/He	Conv. (%)	Product selectivities (%)			
				CO	CO ₂	Alkenes	1,3-butadiene
<i>Oxidation of butane</i>							
Mg ₃ (VO ₄) ₂	540	2/1/22	8.5	13.0	14.0	53.2	12.7
	540	2/1/22	17.0	16.0	20.0	43.3	12.7
Mg ₂ V ₂ O ₇	540	2/1/22	11.1	40.0	33.9	24.5	1.5
	503	2/1/22	17.7	44.2	38.7	15.2	1.9

Even when we were not investigating effects of change in temperature, but lower temperatures gave higher reaction conversions with reduced olefins selectivity. But we can confidently say that our catalyst was better than the Mg catalysts investigated previously by (Kung, 1992). Co₅MgAlO is a better catalyst at lower temperatures than all other previously investigated catalysts because it gives better olefins selectivity at lower temperature of 350°C.

Chapter 6: Conclusion

Short chain paraffin dehydrogenation into Olefins offers a way of turning paraffins into industrially useful hydrocarbon. Theoretically, the concept is simply to comprehend – it is a removal of hydrogen from alkane turning a single bond into a double bonded, alkene. The thermodynamics, kinetic and yield constraints play a critical role for moving this concept from prototype into commercialised system.

The current commercialised processes are energy intensive and give lower yields as the reaction favours the route of chain cleavage into smaller hydrocarbons i.e. methane. Inorganic chemistry in a form of a catalyst has always been used to mitigate the challenges faced by industrial organic chemistry reactions. In addition to the catalyst, partial oxygen introduction to the reaction also has theoretical possibility of moving the reaction from exothermic to endothermic.

Therefore, it is important to know the thermodynamic limits of nature before the catalyst is introduced into the process. For example, the question one would ask is the amount of heat needed (Temperature) to start the dehydrogenation reaction; secondly, one would also need to know how many routes a reaction could take (selectivity). We can answer these questions by calculating the theoretical temperatures needed for each selected route.

We chose to study propane and butane as our alkane hydrocarbons and possible routes were assumed and thermodynamic calculations were done on these assumed routes to calculate the percentage conversions at a certain temperature for a 100% selectivity of the said route. Manipulation of Gibbs free energy, enthalpy and reaction constants for each reaction were used to determine reaction conversions and temperatures at 100 % selectivity. This information is important, as we can know the limits nature is giving us

before we can start rather expensive experimental work thus eliminating trial and error methods.

For propane reactions, we found that it is theoretically possible to run the reaction at lower temperatures our aim being 350°C and reaction % conversion of 20% at 100% selectivity of propene. The challenge is that at these same conditions other routes like total combustion, methane production, ethanol etc. are also possible, giving emphasis to the right catalyst needed to selectively choose the propene production route. Butane also gave similar theoretical thermodynamic and yield results.

Synthesis of catalyst Co_5MgAlO was done in the laboratory and characterised using XRD, TGA and BET for surface structure properties. TPR was conducted to see the reactive properties of the catalyst at different temperatures. The characterisation gave positive results thereby confirming that the catalyst we have synthesised is similar to that which was produced by Marcu (2012).

The reactions were done in a continuous reactor – 1g of the catalyst was added into a reactor – connected to a GC to collect the reaction results data. Temperature of the reactor was maintained at 350°C and atmospheric pressure. The paraffin to oxygen ratio was ranged between; 1:0.4 – 1:1.2.

Butane experimental results at hydrocarbon to oxygen ratio of 1:0.4 gave inconclusive results, while temperature was held constant at 350°C and atmospheric pressure. When oxygen amount was increased the reaction also diverted to produce more carbon dioxide CO_2 , with decreasing alkene selectivity.

A result from this work is the importance of introduction of oxygen thus turning a decades old problem of endothermic dehydrogenation of paraffins to olefins into exothermic reaction. The structural benefit of butane from propane for easy removal of hydrogen can further be investigated. The production of CO_2 from propane can be used

as soft oxidants for dehydrogenation of paraffins as it is currently investigated elsewhere (Wang, 2018).

Historically many processes have been extensively optimised and then replaced; new processes usually go through significant changes to existing technology through research because most evolutionary changes are critical naturally and their effectiveness fade with time. A design will be steadily improved from research to industrial efficiency only to be replaced by fundamentally superior approach (Schmidt, 2000). There is no fixed law of nature that has been realised yet, but could this be the case with endothermic dehydrogenation? Having been around for decades could this be the time for replacement with newer methods of converting paraffins to olefins? The background of process industry is sometimes described as punctuated evolution. Process evolution should continue because scientist and engineers are never fulfilled. They are pushed with the desire to make things better, cheaper and faster.

References

Beretta A., Ranzi E., Forzatti P., Production of olefins via oxidative dehydrogenation of light paraffins at short contact times. *Catalysis Today* 64 (2001) 103 – 111

Beretta A., Ranzi E., Forzatti P., Oxidative dehydrogenation of light paraffins in novel short contact time reactors. Experimental and theoretical investigation, *Chemical Engineering Science* 56 (2001) 779 – 787

Bhasin M.M., McCain J.H., Vora B.V., Imai T., Pujadó P.R., Dehydrogenation and oxydehydrogenation of paraffins to olefins, *Applied Catalysis A: general* 221 (2001) 397 - 419

Blasco T., Galli A., J. M. L'opez. Nieto, and Trifirò F., Oxidative dehydrogenation of Ethane and n – Butane on $\text{VO}_x/\text{Al}_2\text{O}_3$ Catalysts. *Journal of Catalysis* 169 (1997), 203 – 211

Busto M., Benítez V.M., Vera C.R., Grau J.M., Yori J.C., Pt-Pd/ $\text{WO}_3\text{--ZrO}_2$ catalysts for isomerization-cracking of long paraffins, *Applied Catalysis A: General* 347 (2008) 117 – 125

Cavani F., Trifirò F., The Oxydative dehydrogenation of ethane and propane as an alternative way for the production of light olefins. *Catalysis Today* 24 (1995) 307 – 313

Cavani F., Trifiro F., Selective oxidation of light alkanes: interaction between the catalyst and the gas phase on different classes of catalyst materials, *Catalyst Today* 51 (1999) 561 – 580

Cetin E., Odabasi M., Seyfioglu R., Ambient volatile organic compound (VOC) concentrations around a petrochemical complex and a petroleum refinery, *Science of the Total Environment* 312 (2003) 103–112

Degirmenci V., Under D., Yilmaz A., Methane to higher hydrocarbons via halogenation, *Catalysis Today* 106 (2005) 252 – 255

Donald H., Jenkins B. (2008), Chemical Thermodynamics at a Glance, UK, Blackwell Publishing p.g. 56

Dźwigaj S., Gressel I., Grzybowska B., Samson K., Oxidative dehydrogenation of propane on VSi β catalysts. *Catalysis Today* 114 (2006) 237 – 241

Ebbing D.D., Gammon S.D., General Chemistry, Seventh Edition (2002) USA, Houghton Mifflin

Gorimbo J., An experimental and thermodynamic study of iron catalyst activation and deactivation during fischer tropsch synthesis PhD Thesis, University of Witwatersrand, Johannesburg, 2016

Grant J.T., Carrero C.A., Goeltl F., Venegas J., Mueller P., Burt S.P., Specht S.E., McDermott W.P., Chiericato A., Hermans I., Selective oxidative dehydrogenation of propane to propene using boron nitride catalyst. *Et Al., Science* 10.1126/aaf7885 (2016)

Heracleous E., Machli M., Lemonidou A.A., Vasalos I.A., Oxidative dehydrogenation of ethane and propane over vanadium and molybdena supported catalysts. *Journal of Molecular Catalysis A: Chemical* 232 (2005) 29 – 39

Holmen A., Direct conversion of methane to fuels and chemicals, *Catalysis Today* 142 (2009) 2 – 8

<http://www.britannica.com/technology/thermal-cracking> (2015-08-10)

Jiang G., Zhang L., Zhao Z., Zhou X., Duan A., Xu C., Gao J., Highly effective P-modified HZSM-5 catalyst for cracking of C₄ alkanes to produce light olefins, *Applied Catalysis A: General* 340 (2008) 176 – 182

Kung H.H., Kung M.C., The Effect of Potassium in the Preparation of Magnesium Orthovanadate and Pyrovanadate on the Oxidative Dehydrogenation of Propane and Butane, *JOURNAL OF CATALYSIS* 134, 668--677 (1992)

Kung H.H., Kung M.C., Oxidative dehydrogenation of alkanes over vanadium magnesium-oxides, *Applied Catalysis A: General* 157 (1997) 105-116

Lai Y., He S., Luo S., Bi W., Li X., Sun C., Seshan K., Hydrogenation peroxide modified Mg-Al-O oxides supported Pt-Sun catalysts for paraffin dehydrogenation, *Catalysis Communications* 69 (2015) 39 – 42

Lemonidou A.A., Stambouli A.E., Catalytic and non-catalytic dehydrogenation of n – butane. *Applied Catalysis A: General* 171 (1998) 325 – 332

Levels L., PhD Thesis, University of Twente, the Netherlands, 2002

Leveles L., Fuchs S., Fuchs S., Seshan K., Lercher J.A., Lefferts L., Oxidative conversion of light alkanes to olefins over alkali promoted oxide catalysts. *Applied Catalysis A*: 227 (2002) 287 – 297

Li Q., Meng M., Zou Z.Q., Li X.G., Zha Y.Q., Simultaneous soot combustion and nitrogen oxide storage on potassium promoted hydrotalcite – based CoMgAlO catalyst, *Journal of Hazard Materials*: 161 (2009) 366 – 372

Lina T., Sreea U., Tsenga S., Chiub K., Wua C., Loa J., Volatile organic compound concentrations in ambient air of Kaohsiung petroleum refinery in Taiwan, *Atmospheric Environment* 38 (2004) 4111–4122

Lorkovic I.M., Yilmaz A., Yilmaz G.A., Zhou X., Laverman L.E., Sun S., Schaefer D.J., Weiss M., Noy M.L., Cutler C.I., Sherman J.H., McFarland E.W., Stucky G.D., Ford P.C., A novel integrated process for the functionalization of methane and ethane: bromine as mediator, *Catalysis Today* 98 (2004) 317 – 322

Lumen learning (n.d.) Retrieved from <https://courses.lumenlearning.com/boundless-chemistry/chapter/gibbs-free-energy/> accessed (21-07-2019)

Marcu I-C, Pavel O., Tichit D., Acido-basic and catalytic properties of transition-metal containing Mg-Al hydrotalcites and their corresponding mixed oxides, *Applied Clay Science* 61 (2012) 52 – 58

Marcu I-C, Tanasoi S., Mitran G., Tanchoux N., Cacciaguerra T., Fajula F., Sandulescu I, Tichit D., A transition metal-containing mixed oxides catalysts derived from LDH precursors for short-chain hydrocarbons oxidation, *Applied Catalysis A: General* 395 (2011) 78 – 86

Marcu I-C., Sandulescu I., Millet J-M. M., Oxidehydrogenation of n-butane over tetravalent metal phosphates based catalysts, *Applied Catalysis A*: 227 (2002) 309-320

Marcu I-C, Urlan F., Sandulescu I., Oxidative dehydrogenation of n-butane over titanium pyrophosphate catalysts in presence of carbon dioxide, *Catalyst Communications* 9 (2008) 2403 – 2406

Marcu I-C., Urdă A., Herraiz A., Rédey A., Co and Ni ferros spinels as catalysts for propane total oxidation, *Catalysis Communications* 10 (2009) 1651 – 1655

Masuku C.M., Hildebrandt D., Glasser D., Olefin pseudo-equilibrium in the Fischer-Tropsch reaction, *Chemical Engineering Journal* 181 – 182 (2012) 667 – 676

Meng M., Tsubaki N., Li X., Li Z., Xie Y., Hu T., Zhang J., Performance of K-promoted hydrotalcite-derived CoMgAlO catalyst used for soot combustion, NO_x storage and simultaneous soot-NO_x removal, *Applied Catalysis B: Environmental* 91 (2009) 406 – 415

Mitrani G., Cacciaguerra T., Lorient S., Tichit D., Marcu I.-C., Oxidative dehydrogenation of propane over cobalt containing mixed oxides obtained from LDH precursors, *Applied Catalysis A: General* 417 – 418 (2012) 153 – 162

Mølhave L., Bach B., and Pedersen O.E., Human reactions to low concentrations of volatile organic compounds, *Environment International*, Vol. 12, pp. 167-175, 1986

Mølhave L., Jensen J.G. and Larsen S., Subjective reactions to volatile organic compounds as air pollutants, *Atmospheric Environment* Vol. 25A, No. 7, pp. 1283 1293, 1991.

Nawaz Z., Baksh F., Zhu J., Wei F., Dehydrogenation of C₃ – C₄ paraffins to corresponding olefins over slit-SAPO-34 supported Pt-Sn-based novel catalyst, *Journal of Industrial and Engineering Chemistry* 19 (2013) 540 – 546

Owen O.S., Kung M.C. and Kung H.H., The effect of oxide structure and cation reduction potential of vanadates on the selective oxidative dehydrogenation of butane and propane, *Catalysis Letters* 12 (1992) 45-50

Sadykov V.A., Pavlova S.N., Saputina N.F., Zolotarskii I.A., Pakhomov N.A., Moroz E.M., Kuzmin V.A., Kalinkin A.V., Salanov A.N., Danilova I.G., Paukshtis E.A., Olefins formation by oxidative dehydrogenation of propane over monoliths at short contact times, *Studies in Surface Science and Catalysis*, volume 130, (2000) pages 1907 – 1912

Sanfilippo D., Miracca I., Dehydrogenation of paraffins: synergies between catalyst design and reactor engineering, *Catalysis Today* 111 (2006) 133 – 139

Schmidt L.D., Siddall J., Bearden M., New ways to make old chemicals, *AIChE Journal* (2000) 46,8;

Thomas C.L., A history of early cracking research at universal oil products company, *Heterogeneous Catalysis* 222 (2009) pp. 241 – 245

Wang T., Li X., Yan B., Yao S., Kattel S., Chen J.G., Oxidative dehydrogenation and dry reforming of n-butane with CO₂ over NiFe bimetallic catalysts, *Applied Catalysis B: Environmental* 231 (2018) 213 – 223

Appendix

Appendix A: Calculating Enthalpy and Gibbs free energies of formation C₃ and C₄

Table A1: Standard Gibbs free energy G_a , Enthalpy values H_a and Entropy values S_a

<i>Compound</i>	<i>H_a kJ/mol</i>	<i>G_a kJ/mol</i>	<i>S_a kJ/K.mol</i>
C_3H_8	-104.5	-23.4	0.270
C_3H_6	20.2	74.7	0.267
O_2	0	0	0.205
H_2O	-242	-228.61	0.189
CH_4	-74.87	-50.8	0.187
CO	-110.5	-137.23	0.198
CO_2	-393.5	-394.39	0.214
H_2	130	0	0.131
C_3H_4	185.4	194.6	0.248
C_2H_4	52.4	68.1	0.220
C_2H_6	-85	-33	0.230
C_2H_5OH	-235.3	-162.5	0.160
C_4H_{10}	-127.2	-17.0	0.310
C_4H_8	-0.1	71.3	0.305



$$\begin{aligned}
 \Delta H_{rxn}^\emptyset &= \sum Products - \sum Reactants \\
 &= \{(20.2) + (2 \times 249.2) + (2 \times 218)\} - \{(-104.5) + (0)\} \\
 &= 1059.1 \text{ kJ/mol} \\
 \Delta G_{rxn}^\emptyset &= \sum Products - \sum Reactants \\
 &= \{(74.7) + (2 \times 0) + (2 \times 0)\} - \{(-23.4) + (0)\} \\
 &= 98.1 \text{ kJ/mol}
 \end{aligned}$$



$$\begin{aligned}\Delta H_{r \times n}^{\emptyset} &= \sum Products - \sum Reactants \\ &= \{(-0.4) + (2 \times 249.2) + (2 \times 218)\} - \{(-126.5) + (0)\} \\ &= 1060.1 \text{ kJ/mol}\end{aligned}$$

$$\begin{aligned}\Delta G_{r \times n}^{\emptyset} &= \sum Products - \sum Reactants \\ &= \{(72) + (2 \times 0) + (2 \times 0)\} - \{(-15.6) + (0)\} \\ &= 87.6 \text{ kJ/mol}\end{aligned}$$

Appendix B: Calculations of Gibbs free energy of reaction and K_{eq} at 350°C for C_3 and C_4

Assuming that the enthalpy of the reaction remains the same at all temperatures, then we can use the Gibbs – Helmholtz equation to determine Gibbs free energy for the reaction at 350 °C.

$$\frac{G_b}{T_b} = H \left(\frac{1}{T_b} - \frac{1}{T_a} \right) + \frac{G_a}{T_a} \quad (B1)$$

Rearranging the equation at 350°C, then we get;

$$G_b = -1.09H + 2.09G_a \quad (B2)$$

Where H and G_a is the enthalpy and Gibbs free energies calculated in Appendix A and G_b is the Gibbs free energy at 350 °C.

The equilibrium constant is calculated using the equation;

$$K_{eq} = e^{-\frac{G_b}{RT_b}} \quad (B3)$$

G_b and K_{eq} for Propane (C_3)

$$\begin{aligned} G_b &= -1.09H + 2.09G_a \\ &= -1.09(1059.1) + 2.09(98.1) \\ &= -958.2 \text{ kJ/mol} \end{aligned}$$

$$\begin{aligned} K_{eq} &= e^{-\left(\frac{-958.2}{0.008314 \times 623}\right)} \\ &= e^{185.00} = 2.20 \times 10^{80} \end{aligned}$$

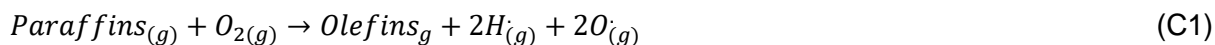
G_b and K_{eq} for Butane (C_4)

$$\begin{aligned} G_b &= -1.09H + 2.09G_a \\ &= -1.09(1060) + 2.09(87.6) \\ &= -972.3 \text{ kJ/mol} \end{aligned}$$

$$\begin{aligned} K_{eq} &= e^{-\left(\frac{-972.3}{0.008314 \times 623}\right)} \\ &= e^{187.72} = 33.4 \times 10^{80} \end{aligned}$$

Appendix C: Equilibrium constant for C₂ – C₅ paraffins to olefins from partial pressures.

Looking at chemical reaction equations in A1, It is evident that the reactions follows similar trends where by;



Assuming that we start with 1 mole of Paraffin and 1 mole of Oxygen, then the products ethene and hydrogen radical and oxygen radical will have product x, x and x respectively at the end of reaction, x is therefore the percentage conversion of the reaction favouring olefins selectivity.

Start of reaction: $1 + 1 \rightarrow 0 + 0 + 0$

End of reaction: $(1 - x) + (1 - x) \rightarrow x + 2x + 2x$

Total concentration at end of reaction is $1 - x + 1 - x + x + 2x + 2x = 2 + 3x$

All equations of C₂ – C₅ follow the same route as the ratio of paraffins for oxygen is the same for all equations.

$$K_{eq} = \frac{[Product]}{[Reactants]} = \frac{[C_2H_4].[H]^2[O]^2}{[C_2H_6].[O_2]} \quad (C2)$$

To find the concentrations of products and reactants we need to apply Dalton's law of partial pressures which is;

$$P_i = y_i P_{Tot}$$

Where P_i = partial pressure of a single gas

y_i = fraction of partial pressure of gas in total number partial pressures of all gases

P_{Total} = total pressure of all gases

$$\text{Therefore; } y_{Olefins} = \frac{x}{2 + 3x} \text{ and;}$$

$$y_{H^+, O^-} = \frac{2x}{2 + 3x} \text{ lastly;}$$

$$y_{paraffins; O_2} = \frac{1 - x}{2 + 3x}$$

Substituting these fractions in equation A2 we get;

$$K_{eq} = \frac{\left(\frac{x}{2+3x}\right)\left(\frac{2x}{2+3x}\right)^4}{\left(\frac{1-x}{2+3x}\right)^2}$$

Simplifying the fraction we get

$$K_{eq} = \frac{16x^5}{(2+3x)^3 \cdot (1-x)^2} \quad (C3)$$

Table C1: K_{eq} calculated with x (% conversion) estimated between 0 – 100%

X	Keq
0	#NUM!
0.1	-649.5475214
0.2	-110.407163
0.3	-27.77861905
0.4	-8.926818796
0.5	-3.972021522
0.6	-2.5202488
0.7	-1.882740188
0.8	-1.231470301
0.9	-0.037647174
1	#NUM!

Appendix D: Calculating ideal temperatures for each % conversions (0 – 100%)

From Table 3 above it is clear that the value of K_{eq} is negative, therefore equation B3 can be written as;

$$-K_{eq} = e^{-\frac{G_b}{RT_b}}$$

The equation can then be simplified as;

$$K_{eq} = -e^{-\frac{G_b}{RT_b}}$$

Applying ln laws then it becomes;

$$\ln(K_{eq}) = -\ln e^{-\frac{G_b}{RT_b}}$$

$$\frac{G_b}{RT_b} = \ln(K_{eq}) \quad (D1)$$

Making T_b subject of the formulae then we get;

$$T_b = \frac{G_b}{R \ln(K_{eq})} \quad (D2)$$

Temperature T_b for C_2 conversions;

Substituting $\Delta H_f = 1071.2$ kJ/mol and $\Delta G_f = 101.1$ kJ/mol in equation B1; then

$$G_b = 1071 \left(1 - \frac{T_b}{298}\right) + \frac{101.1 T_b}{298}$$

$$= 1071 - 3.59T_b + 0.34T_b$$

Therefore in general G_b can be written as;

$$G_b = H \left(1 - \frac{T_b}{298}\right) + \frac{G_a T_b}{298}$$

$$= H - \frac{H}{298} T_b + \frac{G_a}{298} T_b$$

Substituting G_b in equation D2 we get;

$$T_b = \frac{H - \frac{H}{298} T_b + \frac{G_a}{298} T_b}{R \ln(K_{eq})}$$

Making T_b subject of the formulae we get;

$$T_b R \ln(K_{eq}) = H - \left(\frac{H}{298} - \frac{G_a}{298} \right) T_b$$

$$T_b R \ln(K_{eq}) + \left(\frac{H}{298} - \frac{G_a}{298} \right) T_b = H$$

$$T_b = \frac{H}{R \ln(K_{eq}) + \frac{H}{298} - \frac{G_a}{298}}$$

1.1.1. Propane reaction temperature T_b for production of propene

When solving the temperature of the reaction T_b we need to look at Gibbs-Helmholtz equation which is;

$$\frac{\Delta G_b}{T_b} - \frac{\Delta G_a}{T_a} \approx \Delta H_a \left(\frac{1}{T_b} - \frac{1}{T_a} \right) \quad D3$$

Making ΔG_b the subject of the formula and replacing T_a with 298 K the standard temperature from equation 7 above therefore;

$$\Delta G_b = \frac{\Delta G_a T_b}{298} + \Delta H_a - \frac{\Delta H_a T_b}{298} \quad D4$$

Substituting 8 into 2 the equation then becomes;

$$\frac{\Delta G_a T_b}{298} + \Delta H_a - \frac{\Delta H_a T_b}{298} = \Delta G_a + RT_b \ln Q \quad D5$$

Making T_b the propene (olefin) production temperature subject of the formula, it becomes;

$$T_b = \frac{\Delta G_a - \Delta H_a}{(-R \ln Q) - \left(\frac{\Delta H_a}{298} \right) + \left(\frac{\Delta G_a}{298} \right)} \quad D6$$

To solve the temperature ΔT_b value it is clear that we need to calculate the value of Q and the value ΔH_a . ΔH_a is calculated below;

$$\Delta H_a = \sum \text{Products} - \sum \text{Reactants} \quad D7$$

$$= \{(2 \times 20.2) + (2 \times -242)\} - \{(2 \times -104.5) + (0)\}$$

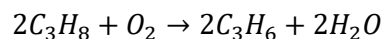
$$= -234.6 \text{ kJ/mol}$$

We need to use the concept of partial pressures at equilibrium to calculate the value of Q .

1.1.2. Using partial pressures to calculate the % conversion from the value of $Q(Kp)$

• Propane (C3) to olefins

Looking at chemical reaction equations 6,



Assuming that we start with 2 mole of Paraffin and 1 mole of Oxygen, and the products are 2 moles of propene and 2 moles of water. The reaction moles distribution will be as follows from beginning to the end of the reaction.

$$\text{Start} : 2 + 1 \rightarrow 0 + 0$$

$$\text{during} : (2 - 2x) + (1 - x) \rightarrow 2x + 2x$$

$$\text{End: } 2 - 2x + 1 - x + 2x + 2x$$

$$\text{Total number of moles at end of reaction: } 3 + x$$

We know that Q can be replaced with K_p going towards equilibrium

$$K_p = \frac{[\text{Product}]}{[\text{Reactants}]} = \frac{[C_3H_6]^2 \cdot [H_2O]^2}{[C_3H_8]^2 \cdot [O_2]} \quad \text{D8}$$

To find the concentrations of products and reactants we need to apply Dalton's law of partial pressures which is;

$$P_i = y_i P_{Tot} \quad \text{D9}$$

Where P_i = partial pressure of a single gas

y_i = fraction of partial pressure of gas in total number partial pressures of all gases

P_{Tot} = total pressure of all gases

$$\text{Therefore; } y_{Olefins; H_2O} = \frac{2x}{3 + x} \text{ and;}$$

$$y_{O_2} = \frac{1 - x}{3 + x} \text{ lastly;}$$

$$y_{paraffins} = \frac{2 - 2x}{3 + x}$$

Substituting these fractions in equation 12 we get;

$$K_p = \frac{\left(\frac{2x}{3+x}\right)^2 \left(\frac{2x}{3+x}\right)^2}{\left(\frac{2-2x}{3+x}\right)^2 \left(\frac{1-x}{3+x}\right)}$$

Simplifying the fraction we get;

$$K_p = \frac{16x^4}{(3+x)(2-2x)^2(1-x)} \quad \text{D10}$$

Assuming that the % conversions run from 0% to 100%; x values can be varied between the fractions 0 – 1 to get the values of K_p (see table below).

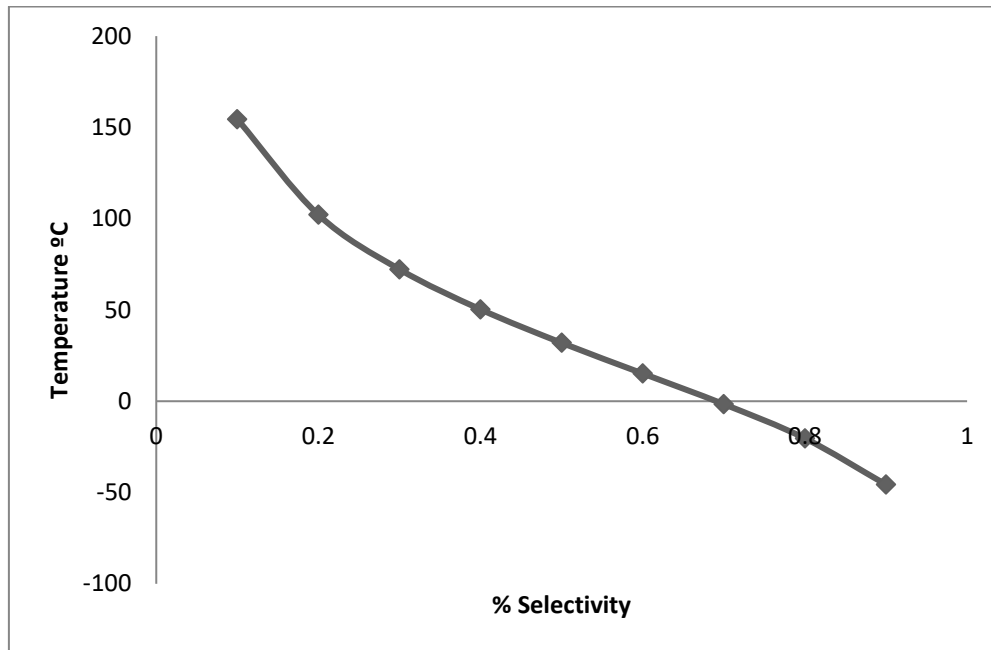
Table D1: Table of % conversions (x) and Value of K_p

x	K_p
0.1	0
0.2	0.000177
0.3	0.003906
0.4	0.028624
0.5	0.139434
0.6	0.571429
0.7	2.25
0.8	9.613614
0.9	53.89474
1	Undefined

Substituting gas constant $R = 0.00831 \text{ kJ/mol.K}$ and K_p into equation 10 the values of the reaction temperature T_b at given % conversion x can be determined.

Table D2: Temperature T_b of reaction for % conversion x of propane to propene

x	K_p	$T_b (K)$	$T_b(^{\circ}C)$
0	0	#NUM!	#NUM!
0.1	0.000177	427.4805	154.4805
0.2	0.003906	375.1075	102.1075
0.3	0.028624	345.2183	72.21834
0.4	0.139434	323.2867	50.28668
0.5	0.571429	304.9708	31.9708
0.6	2.25	288.18	15.18001
0.7	9.613614	271.3794	-1.62058
0.8	53.89474	252.6457	-20.3543
0.9	672.9231	227.3324	-45.6676
1	#DIV/0!	#DIV/0!	#DIV/0!



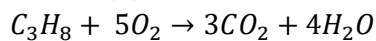
Graph D1: Olefin reaction temperature T_b (°C) vs % conversion x

The data above proves that the olefins can be produced under moderate temperatures. The experimental data have shown that this is not possible as higher temperatures around 800K should be employed to get the results. The other problem that we have is the selectivity, as at these temperatures other reactions are possible (see below).

1.1.3. Other possible reactions temperature T_b and reaction conversion x when propane reacts with oxygen.

G_a was calculated using equation 5 and H_a equation 11

- (1) Combustion



D11

$$\text{Start : } 1 + 5 \rightarrow 0 + 0$$

$$\text{during : } (1 - x) + (5 - 5x) \rightarrow 3x + 4x$$

$$\text{End: } 1 - x + 5 - 5x + 3x + 4x$$

$$\text{Total number of moles at end of reaction: } 6 + x$$

$$K_p = \frac{6912x^7}{(6+x)(1-x)(5-5x)^5}$$

D12

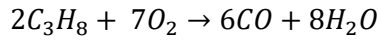
$$G_a = \{(3 \times -394.39) + (4 \times -228.61)\} - \{(-23.4) + 0\}$$

$$= -2074.21 \text{ kJ/mol}$$

$$H_a = \{(3 \times -393.5) + (4 \times -242)\} - \{(-104.5) + 0\}$$

$$= -2044 \text{ kJ/mol}$$

- (2) Incomplete combustion



D13

$$\text{Start : } 2 + 7 \rightarrow 0 + 0$$

$$\text{during : } (2 - 2x) + (7 - 7x) \rightarrow 6x + 8x$$

$$\text{End: } 2 - 2x + 7 - 7x + 6x + 8x$$

$$\text{Total number of moles at end of reaction: } 9 + 5x$$

$$K_p = \frac{7.83 \times 10^{11} x^{14}}{(9+5x)^5 (2-2x)^2 (7-7x)^7}$$

D14

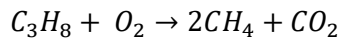
$$G_a = \{(6 \times -137.23) + (8 \times -228.61)\} - \{(2 \times -23.4) + 0\}$$

$$= -2605.46 \text{ kJ/mol}$$

$$H_a = \{(6 \times -393.5) + (8 \times -242)\} - \{(2 \times -104.5) + 0\}$$

$$= -4088 \text{ kJ/mol}$$

- (3) Methane production with CO_2



D15

$$\text{Start : } 1 + 1 \rightarrow 0 + 0$$

$$\text{during : } (1 - x) + (1 - x) \rightarrow 2x + x$$

$$\text{End: } 1 - x + 1 - x + 2x + x$$

$$\text{Total number of moles at end of reaction: } 2 + x$$

$$K_p = \frac{4x^3}{(2+x)(1-x)^2}$$

D16

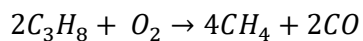
$$G_a = \{(2 \times -50.8) + (-394.39)\} - \{(-23.4) + 0\}$$

$$= -472.59 \text{ kJ/mol}$$

$$H_a = \{(2 \times -74.87) + (-393.5)\} - \{(-104.5) + 0\}$$

$$= -438.74 \text{ kJ/mol}$$

- (4) Methane production with CO



D17

$$\text{Start : } 2 + 1 \rightarrow 0 + 0$$

$$\text{during : } (2 - 2x) + (1 - x) \rightarrow 4x + 2x$$

$$\text{End: } 2 - 2x + 1 - x + 4x + 2x$$

$$\text{Total number of moles at end of reaction: } 3 + 3x$$

$$K_p = \frac{1024x^6}{(3+3x)^3(2-2x)^2(1-x)} \quad \text{D18}$$

$$G_a = \{(4 \times -50.8) + (2 \times -137.23)\} - \{(2 \times -23.4) + 0\}$$

$$= -430.86 \text{ kJ/mol}$$

$$H_a = \{(4 \times -74.87) + (2 \times -110.5)\} - \{(2 \times -104.5) + 0\}$$

$$= -311.48 \text{ kJ/mol}$$

- (5) Alcohol production



$$\text{Start : } 1 + 1 \rightarrow 0 + 0$$

$$\text{during : } (1 - x) + (1 - x) \rightarrow x + x$$

$$\text{End: } 1 - x + 1 - x + x + x$$

$$\text{Total number of moles at end of reaction: } 2$$

$$K_p = \frac{x^2}{(1-x)^2} \quad \text{D20}$$

$$G_a = \{(-162.5) + (-228.61)\} - \{(-23.4) + 0\}$$

$$= -367.71 \text{ kJ/mol}$$

$$H_a = \{(-235.3) + (-242)\} - \{(-104.5) + 0\}$$

$$= -372.8 \text{ kJ/mol}$$

- (6) Other olefins (C_3H_4)



$$\text{Start : } 1 + 1 \rightarrow 0 + 0$$

$$\text{during : } (1 - x) + (1 - x) \rightarrow x + 2x$$

$$\text{End: } 1 - x + 1 - x + x + 2x$$

Total number of moles at end of reaction: $2 + x$

$$K_p = \frac{4x^3}{(2+x)(1-x)^2} \quad \text{D22}$$

$$G_a = \{(194.6) + (2 \times -228.61)\} - \{(-23.4) + 0\}$$

$$= -239.22 \text{ kJ/mol}$$

$$H_a = \{(185.4) + (2 \times -242)\} - \{(-104.5) + 0\}$$

$$= -194.1 \text{ kJ/mol}$$

- (7) Other olefins (C_2H_4)



$$\text{Start : } 1 + 1 \rightarrow 0 + 0 + 0$$

$$\text{during : } (2 - 2x) + (3 - 3x) \rightarrow 2x + 4x + 2x$$

$$\text{End: } 2 - 2x + 3 - 3x + 2x + 4x + 2x$$

Total number of moles at end of reaction: $5 + 3x$

$$K_p = \frac{4096x^8}{(5+3x)^3(2-2x)^2(3-3x)^3} \quad \text{D24}$$

$$G_a = \{(2 \times 68.1) + (4 \times -228.61) + (2 \times -137.23)\} - \{(2 \times -23.4) + 0\}$$

$$= -1005.9 \text{ kJ/mol}$$

$$H_a = \{(2 \times 52.4) + (4 \times -242) + (2 \times -110.5)\} - \{(2 \times -104.5) + 0\}$$

$$= -875.2 \text{ kJ/mol}$$

- (8) Paraffin (C_2H_6)



$$\text{Start : } 1 + 1 \rightarrow 0 + 0 + 0$$

$$\text{during : } (1 - x) + (1 - x) \rightarrow x + x + x$$

$$\text{End: } 1 - x + 1 - x + x + x + x$$

Total number of moles at end of reaction: $2 + x$

$$K_p \frac{x^3}{(2+x)(1-x)^2}$$

D26

$$G_a = \{(-33) + (0) + (-394.39)\} - \{(-23.4) + 0\}$$

$$= -403.99 \text{ kJ/mol}$$

$$H_a = \{(-85) + (-393.5)\} - \{(-104.5) + 0\}$$

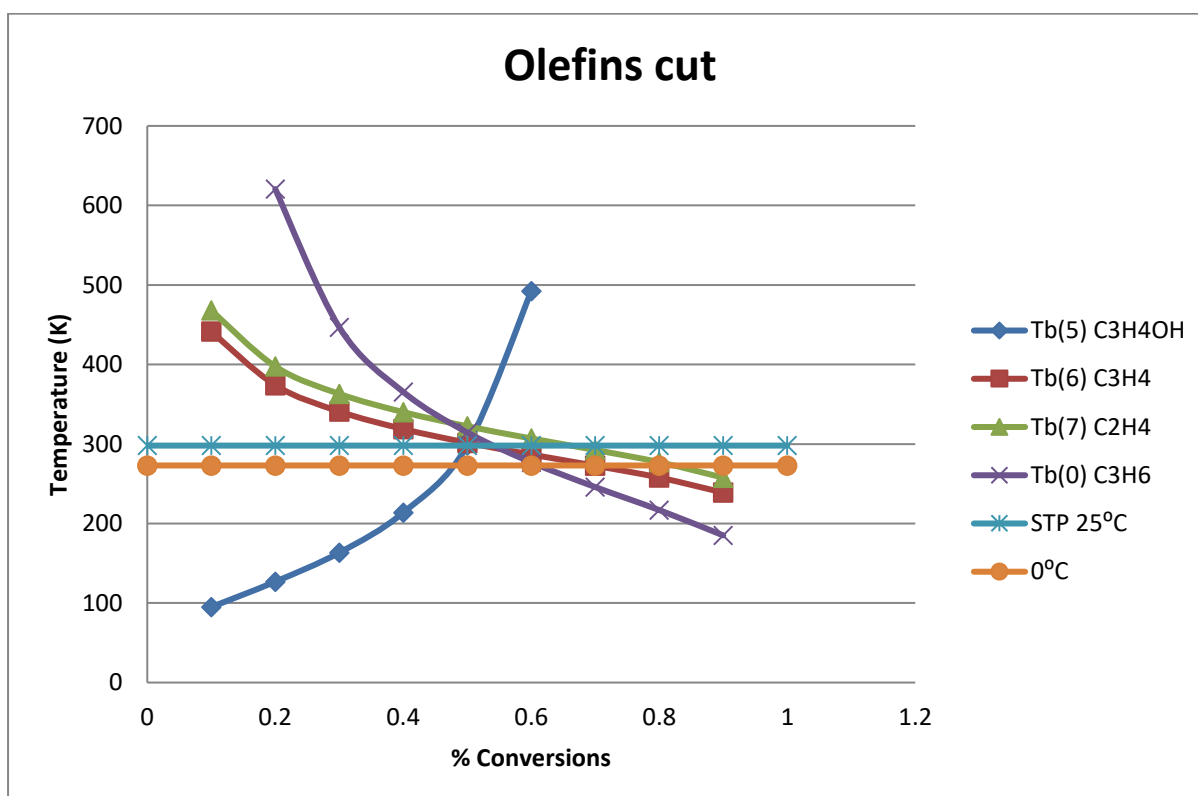
$$= -374 \text{ kJ/mol}$$

Table D3: Table of reaction (1 – 8) H_a and G_a with K_p

Products	H_a kJ/mol	G_a kJ/mol	S_a kJ/K.mol	K_p
(1) $3CO_2 + 4H_2O$	-2044	-2074.21	-0.111	$\frac{6912x^7}{(6+x)(1-x)(5-5x)^5}$
(2) $6CO + 8H_2O$	-4088	-2605.46	0.725	$\frac{7.83 \times 10^{11} x^{14}}{(9+5x)^5(2-2x)^2(7-7x)^7}$
(3) $2CH_4 + CO_2$	-438.74	-472.59	0.088	$\frac{4x^3}{(2+x)(1-x)^2}$
(4) $4CH_4 + 2CO$	-311.48	-430.86	0.201	$\frac{1024x^6}{(3+3x)^3(2-2x)^2(1-x)}$
(5) $C_3H_5OH + H_2O$	-372.8	-367.71	-0.125	$\frac{x^2}{(1-x)^2}$
(6) $C_3H_4 + 2H_2O$	-194.1	-239.22	0.151	$\frac{4x^3}{(2+x)(1-x)^2}$
(7) $2C_2H_4 + 4H_2O + 2CO$	-875.2	-1005.9	0.437	$\frac{4096x^8}{(5+3x)^3(2-2x)^2(3-3x)^3}$
(8) $C_2H_6 + H_2 + CO_2$	-374	-403.99	0.100	$\frac{x^3}{(2+x)(1-x)^2}$

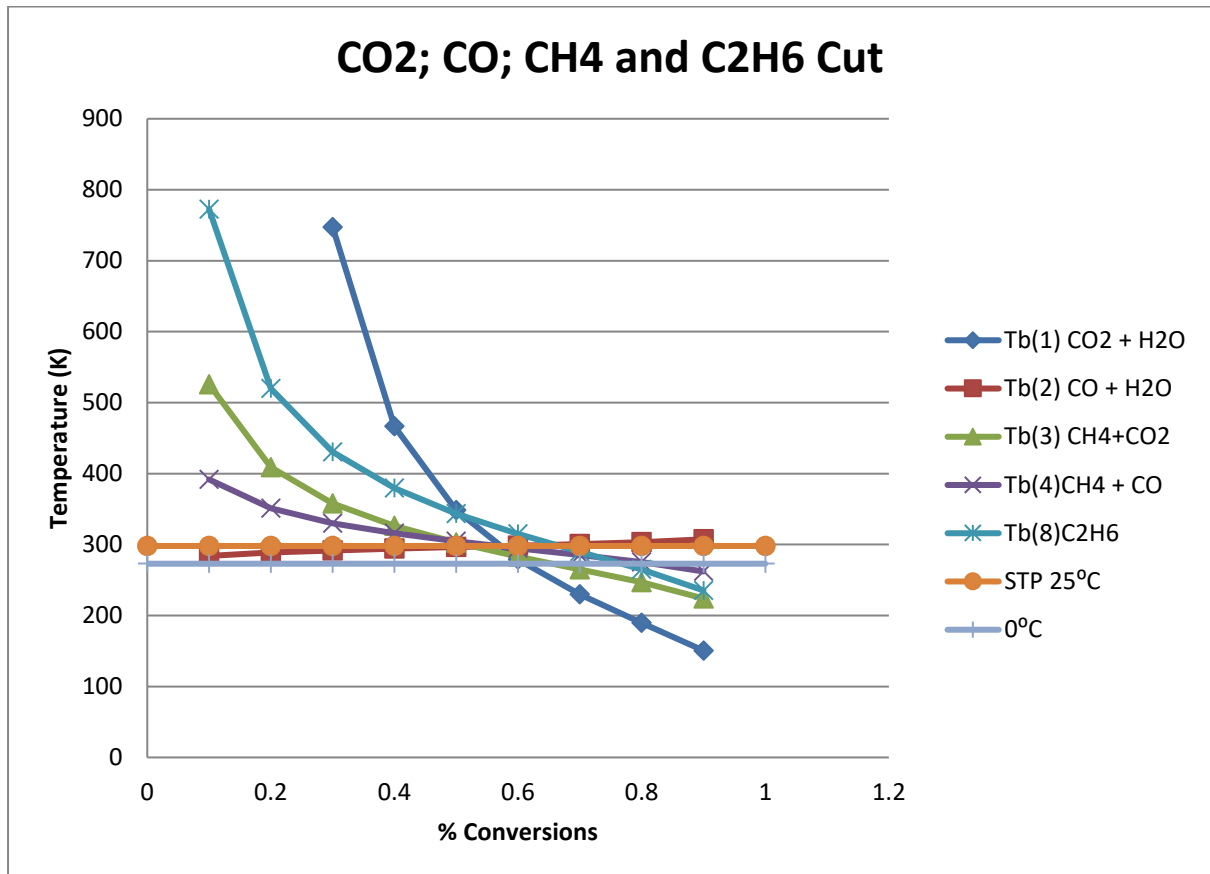
Table D4: Table of % conversion with K_p and T_b values for reaction (1 – 8) C3 paraffins conversions.

x	$K_p(1)$	$K_p(2)$	$K_p(3)$	$K_p(4)$	$K_p(5)$	$K_p(6)$	$K_p(7)$	$K_p(8)$	$T_b(1)$	$T_b(2)$	$T_b(3)$	$T_b(4)$	$T_b(5)$	$T_b(6)$	$T_b(7)$	$T_b(8)$
0	0	0	0	0	0	0	0	0	#NUM!	#NUM!	#NUM!	#NUM!	#NUM!	#NUM!	#NUM!	#NUM!
0.1	6.82E-08	7.93E-14	0.002352	9.77E-06	0.012346	0.002352	4.31E-09	0.000588	-845.213	283.995	525.7653	391.7442	94.9655	441.4824	468.1235	772.5453
0.2	1.74E-05	2.9E-09	0.022727	0.000686	0.0625	0.022727	1.69E-06	0.005682	2928.616	288.7215	408.6923	351.0483	126.867	373.9931	397.5043	520.02
0.3	0.000653	2.21E-06	0.09583	0.009172	0.183673	0.09583	7.21E-05	0.023957	747.2864	291.7876	358.1091	330.1282	163.3367	340.9321	363.0515	430.7113
0.4	0.012136	0.000393	0.296296	0.065524	0.444444	0.296296	0.001341	0.074074	466.8101	294.2283	326.4182	315.8565	213.6917	318.824	340.101	379.5759
0.5	0.170142	0.03693	0.8	0.351166	1	0.8	0.017263	0.2	348.6126	296.4016	302.8366	304.6126	298	301.6139	322.2945	343.6731
0.6	2.290385	2.855531	2.076923	1.6875	2.25	2.076923	0.197842	0.519231	279.044	298.512	283.1861	294.8002	492.1818	286.7465	306.9537	315.0503
0.7	37.29389	268.3779	5.646091	8.409185	5.444444	5.646091	2.513849	1.411523	229.8242	300.7495	265.1505	285.3941	1697.546	272.6578	292.4447	289.7535
0.8	1065.847	54990.62	18.28571	53.27318	16	18.28571	49.06942	4.571429	189.6312	303.414	246.6889	275.2976	-854.073	257.7753	277.1331	264.7718
0.9	153321.2	1.21E+08	100.5517	734.633	81	100.5517	3576.054	25.13793	150.5985	307.3524	224.0603	262.1174	-261.867	238.8639	257.6617	235.3409
1	#DIV/0!	#DIV/0!	#DIV/0!	#DIV/0!	#DIV/0!	#DIV/0!	#DIV/0!	#DIV/0!	#DIV/0!	#DIV/0!	#DIV/0!	#DIV/0!	#DIV/0!	#DIV/0!	#DIV/0!	#DIV/0!



Graph D2: Temperature vs % conversion for olefins cut for C3

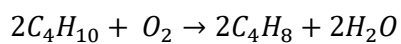
From the graph above it shows clearly that over the temperatures above the STP 25°C the % conversion of propane to olefins is limited by thermodynamics to not go beyond 50% conversions. Then the graph below then goes further to illustrate that there are other reactions possible as Propane reacts with oxygen. This tells us that the catalyst selectivity and ratio of paraffins to olefins in the reactions are very important.



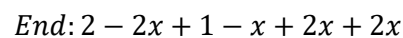
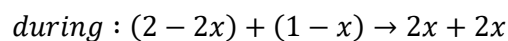
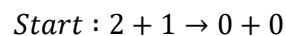
Graph D3: Temperature vs % conversion to CO_2 ; CO ; CH_4 and C_2H_6 cut

- **Butane (C4) to olefins**

For Butane we are only going to look at olefins products when paraffin reacts with oxygen. The following reactions are noted below as the possible routes for reactions.



D27



Total concentration at end of reaction: $3 + x$

$$K_p = \frac{16x^4}{(3+x)(2-2x)^2(1-x)}$$

$$G_a = \{(2 \times 71.3) + (2 \times -228.61)\} - \{(2 \times -17.0) + 0\}$$

$$= -280.62 \text{ kJ/mol}$$

$$H_a = \{(2 \times -0.1) + (2 \times -242)\} - \{(2 \times -127.2) + 0\}$$

$$= -229.8 \text{ kJ/mol}$$



$$Start : 2 + 1 \rightarrow 0 + 0$$

$$during : (2 - 2x) + (1 - x) \rightarrow 4x + 2x$$

$$End: 2 - 2x + 1 - x + 4x + 2x$$

$$Total \text{ concentration at end of reaction: } 3 + 3x$$

$$K_p = \frac{1024x^6}{(3+3x)^3(2-2x)^2(1-x)} \quad D29$$

$$G_a = \{(4 \times 68.1) + (2 \times -228.61)\} - \{(2 \times -17.0) + 0\}$$

$$= -150.82 \text{ kJ/mol}$$

$$H_a = \{(4 \times 52.3) + (2 \times -242)\} - \{(2 \times -127.2) + 0\}$$

$$= -20.4 \text{ kJ/mol}$$



$$Start : 1 + 2 \rightarrow 0 + 0 + 0$$

$$during : (1 - x) + (2 - 2x) \rightarrow x + 2x + x$$

$$End: 1 - x + 2 - 2x + x + 2x + x$$

$$Total \text{ concentration at end of reaction: } 3 + x$$

$$K_p = \frac{4x^4}{(3+x)^1(2-2x)^2(1-x)} \quad D31$$

$$G_a = \{(74.7) + (2 \times -228.61) + (-394.39)\} - \{(2 \times -17.0) + 0\}$$

$$= -742.91 \text{ kJ/mol}$$

$$H_a = \{(20.2) + (2 \times -242) + (-393.5)\} - \{(2 \times -127.2) + 0\}$$

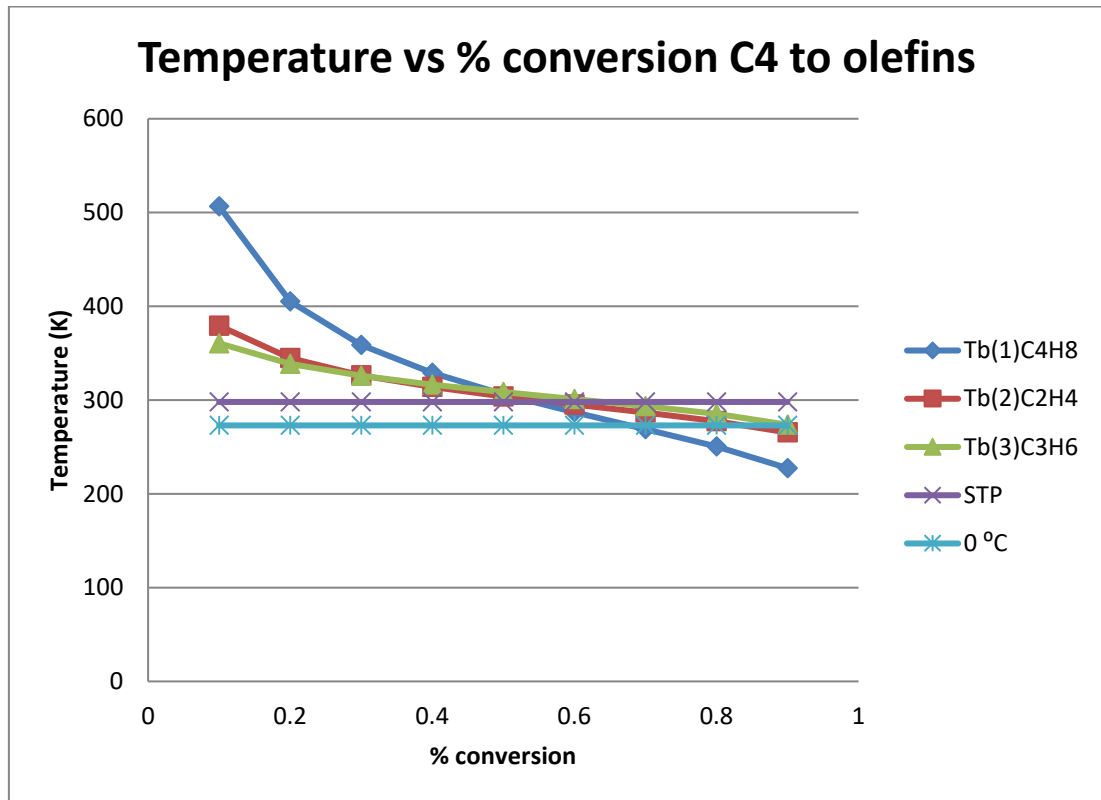
$$= -602.9 \text{ kJ/mol}$$

Table D5: Table of reaction (1 – 3) H_a and G_a with K_p

Products	H_a kJ/mol	G_a kJ/mol	S_a kJ/K.mol	K_p
(1) $2C_4H_8 + 2H_2O$	-229.8	-280.62	0.165	$\frac{16x^4}{(3+x)(2-2x)^2(1-x)}$
(2) $4C_2H_4 + 2H_2O$	-20.4	-150.82	0.433	$\frac{1024x^6}{(3+3x)^3(2-2x)^2(1-x)}$
(3) $C_3H_6 + 2H_2O$ + CO_2	-602.9	-742.91	0.102	$\frac{4x^4}{(3+x)^1(2-2x)^2(1-x)}$

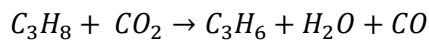
Table D6: Table of % conversion with K_p and T_b values for reaction (1 – 3) C4 paraffins conversions.

X	$K_p(1)$	$K_p(2)$	$K_p(3)$	$T_b(1)C_4H_8$	$T_b(2)C_2H_4$	$T_b(3)C_3H_6$
0	0	0	0	#NUM!	#NUM!	#NUM!
0.1	0.000177	9.77E-06	4.42E-05	211.06846	245.40924	253.94455
0.2	0.003906	0.000686	0.000977	235.69329	262.47966	266.08508
0.3	0.028624	0.009172	0.007156	254.83031	274.11056	274.53334
0.4	0.139434	0.065524	0.034858	272.41388	283.6401	281.64212
0.5	0.571429	0.351166	0.142857	290.25638	292.3173	288.29258
0.6	2.25	1.6875	0.5625	309.9838	300.92502	295.06232
0.7	9.613614	8.409185	2.403403	334.04046	310.27293	302.59142
0.8	53.89474	53.27318	13.47368	367.9347	321.76193	312.04297
0.9	672.9231	734.633	168.2308	432.15259	339.63708	327.00146
1	#DIV/0!	#DIV/0!	#DIV/0!	#DIV/0!	#DIV/0!	#DIV/0!



Graph D3: Temperature vs % conversion for olefins cut for C4

Using Carbon dioxide (CO₂) as soft Oxidant for propane ODH



Start : 1 + 1 → 0 + 0 + 0

during : (1 - x) + (1 - x) → x + x + x

End: 2 - x

Total concentration at end of reaction: 3 + 3x

$$K_p = \frac{x^3}{(2+x)(1-x)^2}$$

D32

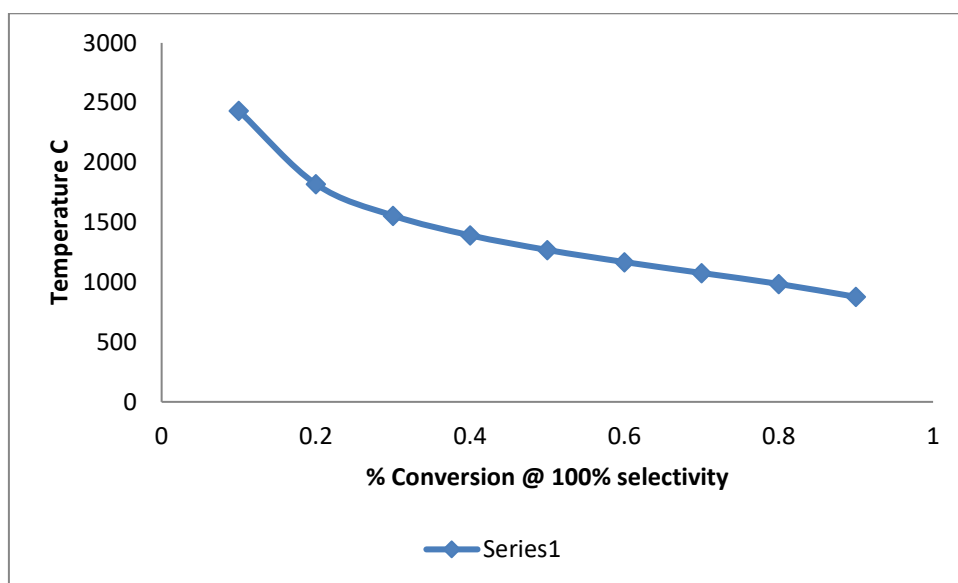
$$G_a = \{(74.7) + (-137.23) + (-228.61)\} - \{(-23.4) + (-393.5)\}$$

$$= 125.76 \text{ kJ/mol}$$

$$H_a = \{(20.2) + (-110.5) + (-245)\} - \{(-104.5) + (-393.5)\}$$

$$= 162.7 \text{ kJ/mol}$$

X	Kp	Tb K	Tb C
0	0	#NUM!	#NUM!
0.1	0.00065	2706.376	2433.376
0.2	0.006944	2092.867	1819.867
0.3	0.032413	1829.471	1556.471
0.4	0.111111	1664.691	1391.691
0.5	0.333333	1542.498	1269.498
0.6	0.964286	1441.487	1168.487
0.7	2.931624	1350.11	1077.11
0.8	10.66667	1258.714	985.7143
0.9	66.27273	1150.525	877.5251
1	#DIV/0!	#DIV/0!	#DIV/0!



Appendix E

Run 2

Run 3

Reactants			Products			
	Propane	Oxygen	C ₂ H ₆	CO ₂	Propane	Oxygen
Area	68011.25	2547.73	14.345	1376.086	13163.04	6.70755
Response Factor	0.68	0.8	0.59	0.915	0.68	0.8
Corrected Area	100016.54	3184.73	24.31	1503.92	19357.41	8.38

	Ratio of Propane to Oxygen		
	Run 1 1:0.4	Run 2 1:0.8	Run 3 1:1.2
<i>Conversion,</i>		%	%
C ₃ H ₈	-	80.64	99.73
O ₂	-	99.73	87.41
<i>Product selectivity,</i>		%	%
C ₂ H ₄	-	0	0.60
C ₂ H ₆	-	1.59	3.92
CO ₂	-	98.00	95.49

Calibration of Butane gas (C₄H₁₀)

Figure E1: Calibration graph of Butane

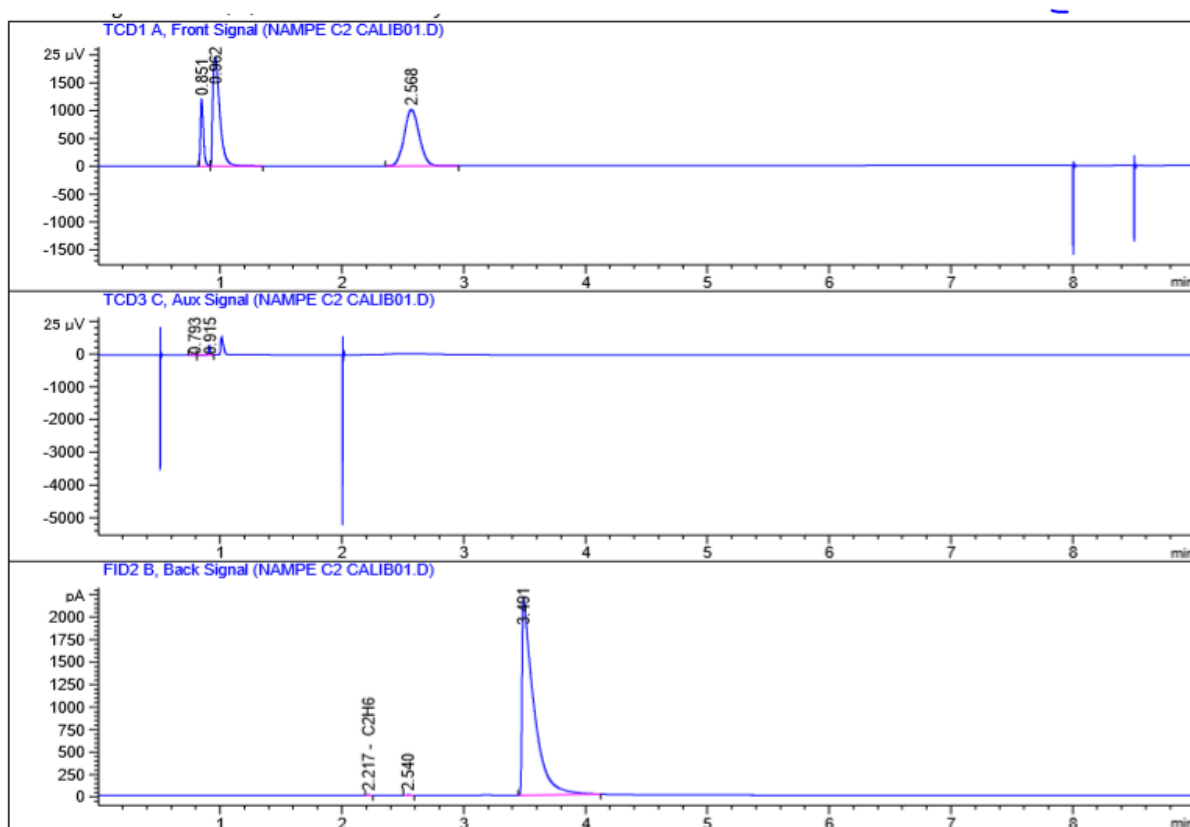


Table E1: Pure Butane composition

Compound	Ret time	Run 1	Run 2	Average Area	Composition % mol
C ₂ H ₆	2.21	Area	Area	3.715051	0.03
C ₄ H ₁₀	3.49	4.050874	3.379335	14667.49	99.97
		14672.89	14662.08		

$$\text{Corrected C}_4\text{H}_{10} \text{ area} = \frac{14667.49}{0.68} = 21569.84$$

Figure E2: Calibration of Air

Data File C:\CHEM32\1\DATA\INSTRUMENT1_2017_FEB\INSTRUMENT1 2019-02-01 14-29-44\NAMPEAIRCAL1.D
Sample Name: NAMPEAIRCAL

```
=====
Acq. Operator   : SYSTEM                      Seq. Line :    1
Acq. Instrument : Instrument1                 Location  : Vial 5
Injection Date  : 2/1/2019 14:30:07          Inj       :    1
                                           Inj Volume: 1000 µl

Sequence File   : C:\Chem32\1\DATA\Instrument1_2017_Feb\INSTRUMENT1 2019-02-01 14-29-44
                  \INSTRUMENT1.S
Method          : C:\CHEM32\1\DATA\INSTRUMENT1_2017_FEB\INSTRUMENT1 2019-02-01 14-29-44
                  \INSTRUMENT1_INLET.M (Sequence Method)
Last changed    : 2/1/2019 14:29:44 by SYSTEM
```

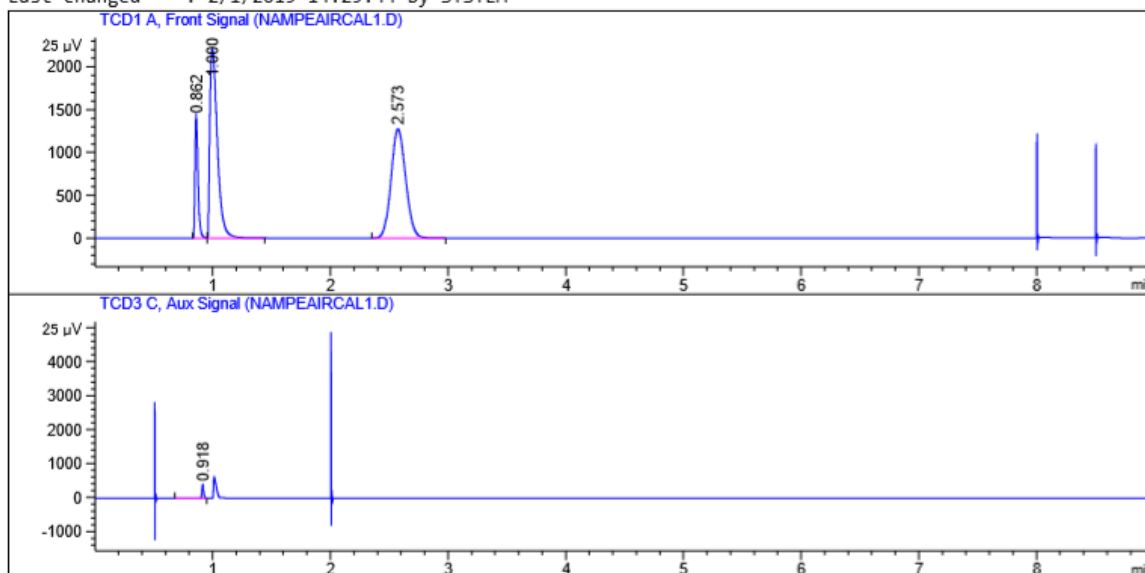


Table E2: Pure Air composition

Compound	Run 1		Run 2		Run 3		Average Area
	RetTime	Area	RetTime	Area	RetTime	Area	
O ₂	0.8	2527.2	0.86	2541.6	0.8	2555.5	2541.4
N ₂	0.9	9795.2	1.00	9840.3	1.0	9891.4	9842.3

$$\text{Corrected O}_2 \text{ area} = \frac{2541.4}{0.8} = 3176.75$$

Figure E3: Reaction composition of Butane and air at ratio 1:04

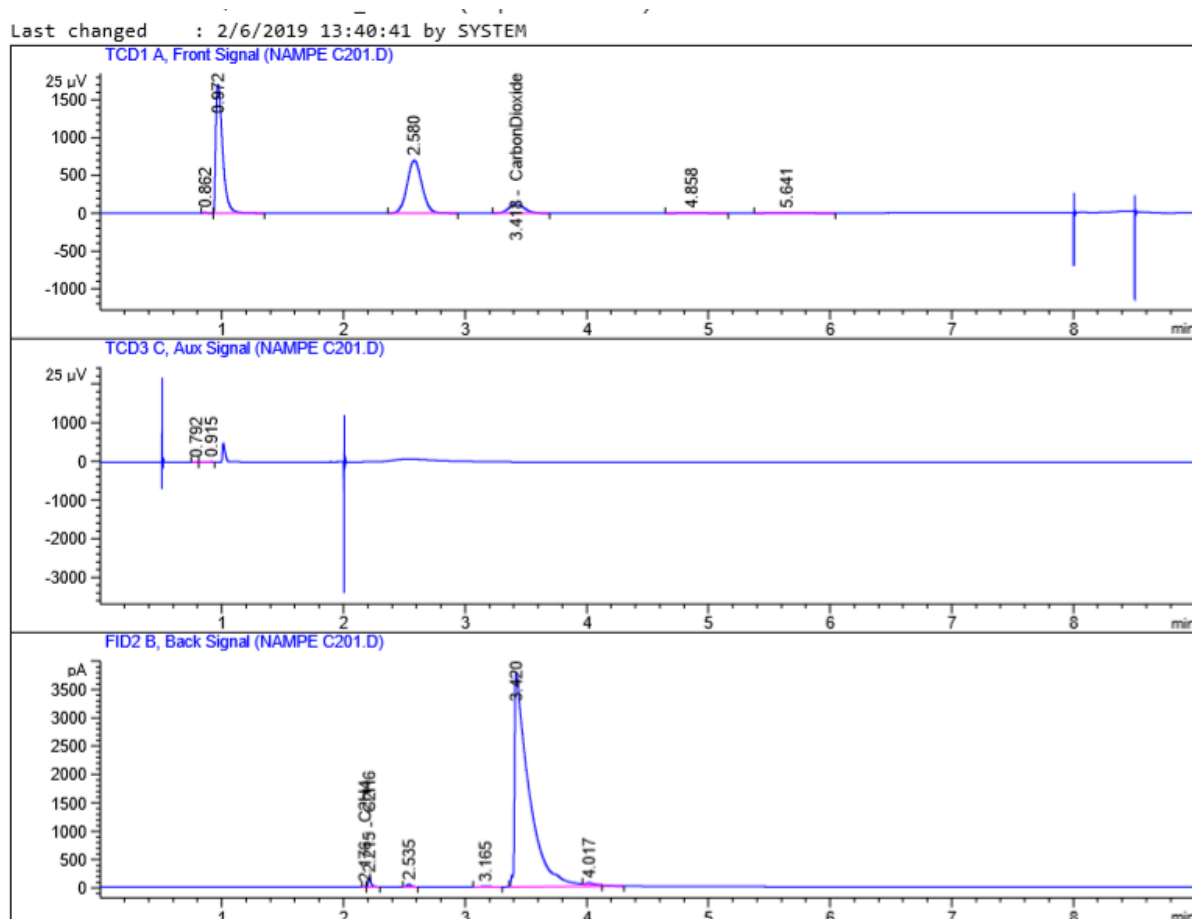


Table 3: Reaction of Butane with Oxygen 1:0.4 ratio

Compound	Ret Time	Run 1	Run 2	Run 3	Run 4	Average Area
O ₂	0.80	6.484	2.984	5.342	4.779	4.897
CO ₂	3.41	1056.3	1052.4	1051.3	1054.8	1053.7
C ₂ H ₄	2.17	5.03	5.08	5.22	5.25	5.15
C ₂ H ₆	2.22	37.57	30.46	26.19	16.19	27.60
1-C ₄ H ₈	3.42	32315.78	32283.61	32392.31	32389.04	32360.19

Figure E5: Reaction composition of Butane and air at ratio 1:0.8

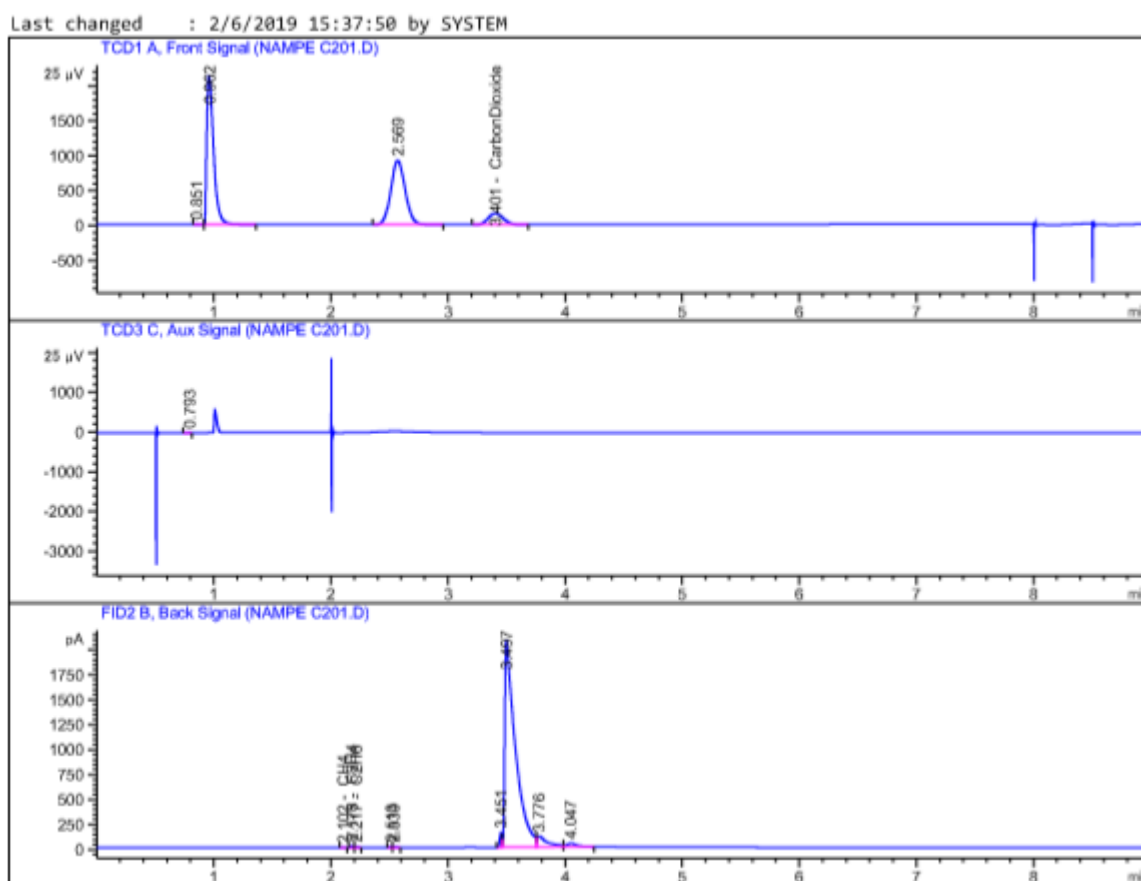


Table E4: Reactions of Butane with Oxygen 1:0.8 ratio

Compound	Ret Time	Run 1	Run 2	Run 3	Run 4	Average Area
O ₂	0.80	6.763	6.969	6.658	6.504	6.724
CO ₂	3.41	1449.25	1449.46	1448.50	1450.49	1449.42
C ₂ H ₄	2.17	26.30	27.31	27.10	26.85	26.89
C ₂ H ₆	2.22	10.77	9.86	10.06	9.77	10.12
1-C ₄ H ₈	3.42	214.482	215.34	215.63	215.53	215.25
C ₄ H ₁₀	3.49	12963.3	12981.1	12898.0	12859.8	12925.6

Table E5: Reactions of Butane with Oxygen 1:0.8 ratio with corrected areas

Compound	Average Area	Response factor	Corrected Area
O ₂	6.724	0.8	8.41
CO ₂	1449.42	0.915	1584.07
C ₂ H ₄	26.89	0.585	45.97
C ₂ H ₆	10.12	0.59	17.15
1-C ₄ H ₈	215.25	0.697	308.82
C ₄ H ₁₀	12925.6	0.68	19008.23

$$\text{Corrected Area} = \frac{\text{Area}}{Rs (\text{response factor})}$$

$$\% \text{ Conversion} = \left[\frac{\text{Initial} - \text{Final}}{\text{Initial}} \right] \times 100\%$$

Figure E5: Reaction composition of Butane and air at ratio 1:1.2

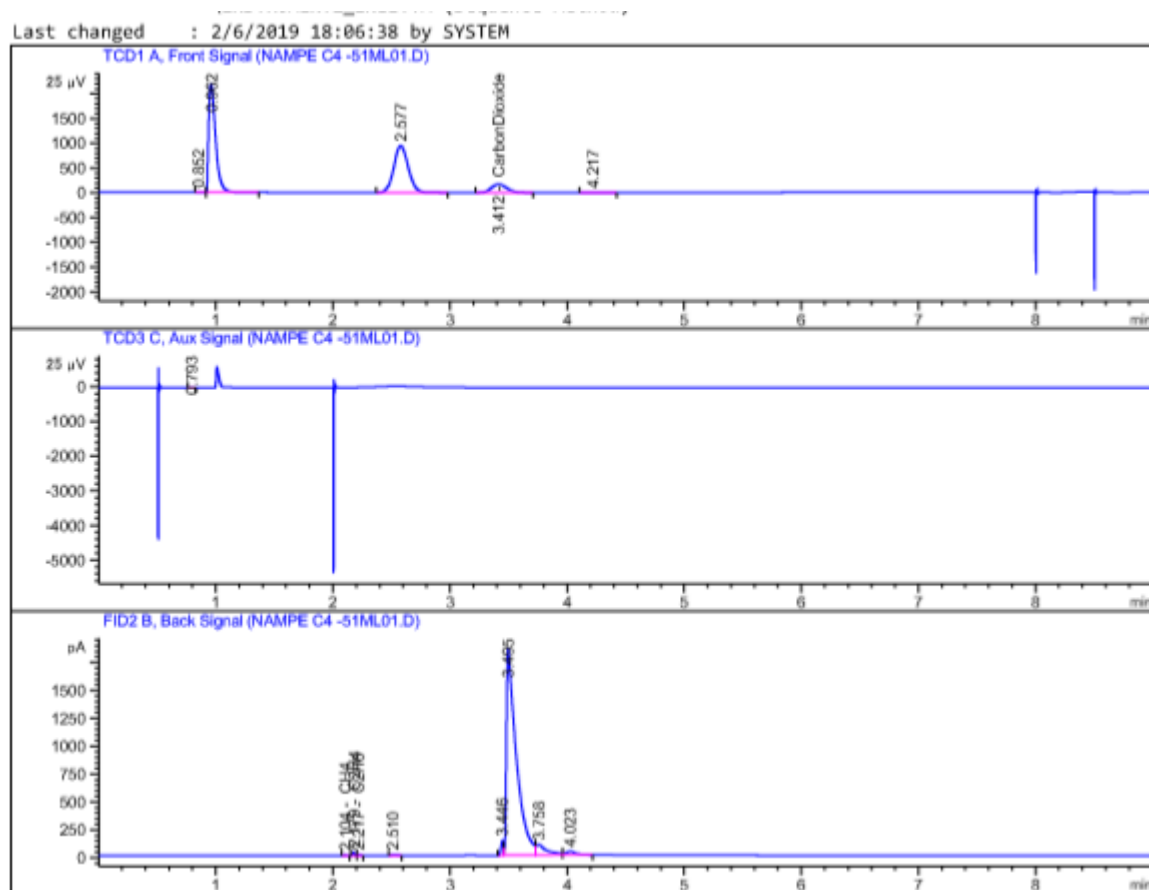


Table E5 Reactions of Butane with Oxygen 1:1.2

Compound	Ret Time	Run 1	Run 2	Run 3	Run 4	Average Area
O ₂	0.80	6.523	6.490	6.645	6.705	6.591
CO ₂	3.41	1521.70	1526.56	1528.26	1532.95	1527.67
C ₂ H ₄	2.17	43.71	43.79	43.66	44.00	43.79
C ₂ H ₆	2.22	12.42	12.03	13.71	12.70	12.72
1-C ₄ H ₈	3.42	217.68	219.57	221.17	220.28	219.68
C ₄ H ₁₀	3.49	10866.0	10830.0	10833.0	10812.2	10835.3

Compound	Average Area	Response factor	Corrected Area
O2	6.591	0.8	8.239
CO2	1527.67	0.915	1669.58
C2H4	43.73	0.585	74.75
C2H6	12.72	0.59	21.56
1-C4H8	219.68	0.697	315.18
C4H10	10835.3	0.68	15934.27

Table E6: Conversion % of Olefins and Oxygen and Product selectivity % for Oxy-dative dehydrogenation reaction

	Ratio of Butane to Oxygen		
	1:0.4	1:0.8	1:1.2
<i>Conversion</i>	%	%	%
C ₄ H ₁₀	-	11.92	26.16
O ₂	-	99.74	99.74
<i>Product selectivity</i>	%	%	%
C ₂ H ₄	-	1.58	2.43
C ₂ H ₆	-	0.59	0.71
CO ₂	-	85.18	84.67
1-C ₄ H ₈	-	12.65	12.19